AN INVESTIGATION OF THE FEASIBILITY OF OBTAINING LATERAL STABILITY DERIVATIVES FOR A LINEAR AIRCRAFT BY MATCHING ANALOG COMPUTER TRANSIENT RESPONSES TO FLIGHT TEST DATA

R. C. Adams
C. R. Cooper
T. F. Dedman

15

AN INVESTIGATION OF THE FEASIBILITY OF OBTAINING LATERAL STABILITY DERIVATIVES FOR A LINEAR AIRCRAFT BY MATCHING ANALOG COMPUTER TRANSIENT RESPONSES TO FLIGHT TEST DATA

R. C. Adams, Lieutenant, USN
C. R. Cooper, Lieutenant, USN
T. F. Dedman, Lieutenant, USN

Aeronautical Engineering Report No. 384
June 1, 1957

Submitted in partial fulfillment of the requirements for the degree of Master of Science in Engineering from Princeton University, June, 1957.

ACKNOWLEDGEMENTS

The authors wish to express their appreciation to Professor Edward Seckel and Mr. Enoch J. Durbin, of the Department of Aeronautical Engineering of Princeton University, for their very considerable assistance, ideas, and guidance throughout the conduct of this investigation. The very great personal interest of Professor Seckel in the nature of the fundamental problem, and his careful analysis of the progress of the solution, were invaluable to the authors, especially during the planning of the flight test program, and the evaluation of the test data. Mr. Durbin and his Instrumentation Laboratory staff contributed a great deal of time and patience in assisting with the design and development of the instrumentation and data analysis systems, and with the solution to many problems in connection with their use.

Appreciation is also expressed to Princeton University for making available the excellent facilities for conducting this type of flight research. In this particular, the authors wish to thank Mr. Robert R. Cooper and the other members of the hangar staff for their assistance in the installation of the test instrumentation, and for the excellent maintenance of the test aircraft.

35762

The authors also wish to acknowledge the very great contribution to the success of this project made through the loan of flight test equipment from the Instrumentation Laboratory of the Flight Test Division of the Naval Air Test Center, Patuxent, Maryland.

AN INVESTIGATION OF THE FEASIBILITY OF OBTAINING LATERAL STABILITY DERIVATIVES FOR A LINEAR AIRCRAFT BY MATCHING ANALOG COMPUTER TRANSIENT RESPONSES TO FLIGHT TEST DATA

SUMMARY

Using a North American NAVION as a flight test vehicle, and an electronic analog computer as a simulator, a study was made of the feasibility of obtaining certain lateral stability derivatives by matching the transient responses of an analog computer on which the lateral operational equations of motion for a NAVION aircraft were set up, to the actual airplane lateral response in sideslip angle, roll rate, and yaw rate.

The matching process was achieved by supplying time histories of the actual recorded control motions as forcing function inputs to the computer, and systematically varying those coefficients of the analog which corresponded to the stability derivatives of the dynamic equations of motion.

The method was demonstrated to be a practical procedure for obtaining the lateral stability derivatives of a linear aircraft. The use of four different types of control deflections as forcing functions provided a means for matching of computer responses which corresponded to a wide range of flight maneuvers.

The method is considered suitable for further investigation, and development for use under different flight conditions and with non-linear aircraft.

TABLE OF CONTENTS

Page

Summary iii

Table of Symbols ix

Introduction 1

Equipment and Procedure 5

  Equipment 5

    Airborne Instrumentation 5
    Ground Station Instrumentation 13
    Instrument Calibration 14

  Procedure 18

    Airborne Phase 18
    Ground Station 22
    Data Reduction 23

Discussion 26

  General Description of Overall Program 26

  Preliminary Considerations 27

    Theoretical Background 27
    Practical Aspects 30

  Analog of the Test Aircraft 32

    Theoretical Approximation of Stability Derivatives 32
    Lateral Equations of Motion 32

  Development of Method of Analysis 34

  Preliminary Test of Feasibility of Method 36

  Application of Method to Flight Test Data 37

TABLE OF CONTENTS (Continued)

Page

Results 46

Conclusions and Recommendations 50

References 52

Tables

Figures

Appendix A Dynamic Response of Sideslip Vane A-1

Appendix B Determination of Lateral Stability Derivatives for the NAVION from Theoretical Formulae and from Wind Tunnel and Flight Tests of Geometrically Similar Airplanes B-1

Appendix C Corrections to Recorded Aileron Data C-1

TABLES

I. Methods for Analysis of Dynamic Flight Test Data.

II. Physical Characteristics of Test Aircraft.

III-a. Effect of Variation of Stability Derivatives on Aircraft Response.

III-b. Stability Derivatives Which Influence Specific Aspects of Aircraft Response.

IV. Primary Effects of Individual Stability Derivatives on Aircraft Response.

V. Comparison of Theoretical and Final Experimental Lateral Stability Derivatives for the NAVION Aircraft.

FIGURES

1. Three-View Drawing of Test Aircraft.

2. Photograph of Test Aircraft.

3. Circuit Diagram for Dynamic Flight Test Instrumentation System of Test Aircraft.

4. Photograph of Sideslip Vane.

5. Instrumentation System Signal Circuit Schematic.

6. Photograph of Aircraft Instrumentation.

7. Elements of a Pulse Width Data Collection System.

8. Photograph of Ground Station Equipment.

9. Calibration of Roll and Yaw Rate Gyros.

10. Static Calibration of Sideslip Vane Potentiometer.

11. Analog of NAVION Lateral Equations of Motion.

12. Potentiometer Settings for Analog of NAVION.

13. Computer Forcing Function Circuits.

14. Initial Response to Rudder Pulse, Theoretical Derivatives.

15. Matched Response to Rudder Pulse, Final Configuration.

16. Matched Response to Rudder Doublet, Final Configuration.

17. Matched Response to Aileron Doublet, Final Configuration.

18. Matched Response to Aileron Step Function, Final Configuration.

A-1. Dynamic Response of Sideslip Vane.

SYMBOLS

CAPITAL LETTERS

AR	Aspect Ratio, b^2/S
CG	Center of Gravity
C_L	Lift Coefficient, Lift/qs
C_D	Drag Coefficient, Drag/qs
C_m	Pitching Moment Coefficient, $\text{Pitching Moment}/qs$
C_ℓ	Rolling Moment Coefficient, $\text{Rolling Moment}/qsb$
C_n	Yawing Moment Coefficient, $\text{Yawing Moment}/qsb$
C_y	Lateral Force Coefficient, $\text{Lateral Force}/qs$

$$C_{L_\alpha} = \frac{\partial C_L}{\partial \alpha}$$

$$C_{m_\alpha} = \frac{\partial C_m}{\partial \alpha}$$

$$C_{\ell_\beta} = \frac{\partial C_\ell}{\partial \beta}$$

$$C_{n_\beta} = \frac{\partial C_n}{\partial \beta}$$

$$C_{y_\beta} = \frac{\partial C_y}{\partial \beta}$$

$$C_{\ell_p} = \frac{\partial C_\ell}{\partial \frac{pb}{2V}}$$

$$C_{n_p} = \frac{\partial C_n}{\partial \frac{pb}{2V}}$$

$$C_{Y_{\delta_r}} = \frac{\partial C_Y}{\partial \delta_r}$$

$$C_{\ell_{\delta_r}} = \frac{\partial C_\ell}{\partial \delta_r}$$

$$C_{n_{\delta_r}} = \frac{\partial C_n}{\partial \delta_r}$$

$$C_{\ell_{\delta_a}} = \frac{\partial C_\ell}{\partial \delta_a}$$

$$C_{n_{\delta_a}} = \frac{\partial C_n}{\partial \delta_a}$$

C_{l_r}	$= \frac{\partial C_l}{\partial \frac{rb}{2V}}$
C_{n_r}	$= \frac{\partial C_n}{\partial \frac{rb}{2V}}$
D	Differential Operator, $d/d\ t/\tau$ Also, propeller diameter, ft.
I_x	Moment of Inertia about X axis, slug ft.^{2}
I_z	Moment of Inertia about Z axis, slug ft.^{2}
J_x	Non-Dimensional Inertia Factor, $2\frac{I_x}{mb^2}$
J_z	Non-Dimensional Inertia Factor, $2\frac{I_z}{b^2m}$
P	Period of Lateral Oscillation, seconds
S	Wing Area, ft.^{2}
S_x	Characteristic Area (See appropriate subscript)
$T_{\frac{1}{2}}$	Time to damp to one-half amplitude, sec.
T_c	Thrust Coefficient
V_i	Indicated airspeed, miles per hour
V	True airspeed, ft/sec.
W	Aircraft Test Weight

LOWER CASE LETTERS

a	Lift Curve Slope, per radian
b	Wing Span, ft
c	Wing Chord, ft
$\bar{c}$	Mean Aerodynamic Chord, ft
e	Airplane Efficiency Factor
g	Acceleration Due to Gravity, ft/sec^2
h_d	Density Altitude, ft
h_p	Pressure Altitude, ft
ℓ_{vt}	Vertical Tail Length; distance from center of pressure of vertical tail to CG, ft
ℓ_{sv}	Sideslip Vane Length; distance from sideslip nave pivot to aircraft CG, ft
m	Mass of Airplane, slugs
p	Rolling Velocity, $\text{radians}/\text{sec}$
q	Dynamic Pressure, $\rho/2\, V^2$, lb/ft^2
r	Yawing Velocity, rad/sec
t	Time, seconds
z_{vt}	Vertical Tail Height; distance from center of pressure of Vertical Tail to X axis

SUBSCRIPTS

a	Aileron
fus	Fuselage
p	Propeller
r	Rudder
vt	Vertical Tail
w	Wing
$\dot{x}$, $\ddot{x}$	Denote First and Second Derivatives with Respect to Real Time

GREEK LETTERS

α	Angle of Attack of Longitudinal Body Axis, deg.
β	Angle of Sideslip, radians
γ	Flight Path Angle, deg.
δ	Control Surface Deflection
ζ	Damping Ratio
η_{vt}	Vertical Tail Efficiency Factor
λ	Taper Ratio, Tip Chord/Root Chord
μ	Relative Density Factor, $m/\rho sb$
ρ	Mass Density of Air
τ	Time Conversion Factor, $m/\rho sV$
ϕ	Angle of Bank, radians
ψ	Angle of Yaw, radians
ω	Angular Frequency, radians/sec
ω_n	Natural Frequency, radians/sec
Γ	Dihedral Angle, degrees
Λ	Sweepback of Wing Quarter-Chord Line, degrees

INTRODUCTION

Since the close of World War II, and the advent of the high speed and altitude characteristics of jet aircraft, the need for a quantitative knowledge of the dynamics of flight has resulted in rapid development of the field of aircraft dynamics. The past six or seven years, in particular, have brought considerable progress in the field of dynamic stability flight testing of aircraft and missiles. The early theoretical and experimental investigations in this area by the Cornell Aeronautical Laboratory, and by the Instrumentation Laboratory of the Massachusetts Institute of Technology, have been supplemented on many fronts, and in particular, by the NACA, which in recent years has developed its dynamic stability testing techniques to the point where free-flight testing of rocket powered and telemeter equipped models has become commonplace.

The role of full scale dynamic flight testing is twofold. First, it provides a designer with the conventional data on the characteristics of an aircraft for the particular conditions of the test. Secondly, and in the long view, more importantly, dynamic flight testing provides a means for solution of the inverse problem of dynamics, wherein the equations describing a system are assumed known, its output in response to suitable forcing functions is measured, and thus the coefficients of the equations, or stability derivatives, can be determined.

Once established, these stability derivatives are of considerable value. They are indispensable to the aerodynamicist who must calculate stability characteristics over a wide range of flight conditions, and who is thus provided with a measure of the accuracy of the theoretical and empirical derivatives used in preliminary design calculations. Determination of the stability derivatives from flight tests also aids the designer by indicating lines along which the stability may be improved, either by geometric design changes, or by artificial augmentation. In the latter regard, the successful design of any system for automatic control of an aircraft is greatly dependent upon an accurate knowledge of the stability derivatives of the airplane.

The basic approaches to the problem of the determination of stability derivatives from dynamic flight testing, and in particular, from experimental time histories, can be separated into two categories - the "equations of motion" method, which essentially solves the inverse problem described above, and a second category, "response curve fitting," which identifies a collection of methods using various mathematical and graphical concepts to extract from the data certain combinations of stability derivatives and inertia terms called transfer function coefficients. All of the individual methods which make up the above two categories will not be described in this report, but an excellent discussion of each current method can be found in Ref. 1. Table I presents a summary and comparison of these various methods for

analysis of dynamic systems. As can be seen from Table I, the choice of a method for analyzing dynamic response data will depend primarily on whether transfer functions, or actual stability derivatives are desired.

Several investigations have been reported (ie, Ref. 2) which have attempted to obtain stability derivatives by applying a particular combination of the above referenced methods which essentially involved the conversion of time response to frequency response, followed by a matching process which utilized both dynamic response templates and an analog computer to produce transfer function coefficients. These constants were then shown to uniquely determine the time response of an analog of the test airplane which accurately duplicated the time history of the actual test vehicle. Evaluation of the actual aerodynamic stability derivatives, however, required supplemental calculations, and was possible only in the case of those derivatives which exerted the strongest influence on the airplane response.

The major limitations of the above method are the length of time required for conversion of the flight data from time response to frequency response form, and the necessity for the subsequent use of templates to determine approximate transfer function coefficients. It was considered that both of these limitations could be avoided in the application of the above method if the matching process were to be applied directly to the transient flight data.

This report, then is concerned with a study of the feasibility of obtaining certain lateral stability derivatives by matching the transient responses from an analog computer on which the operational equations for a NAVION aircraft were set up, to the actual airplane lateral response in sideslip angle, roll rate, and yaw rate. The matching process was achieved by supplying time histories of the actual recorded control motions as inputs to the computer, and systematically varying those coefficients of the analog which corresponded to the stability derivatives of the dynamic equations of motion.

An additional objective of this investigation was to determine the suitability of a pulse width telemeter system as a data collecting scheme for a dynamic flight test program requiring very accurate determination of the recorded quantities.

This investigation was carried out at the James Forrestal Research Center, Princeton University, Princeton, New Jersey, during the 1956-57 academic year.

EQUIPMENT AND PROCEDURE

EQUIPMENT

Airborne Instrumentation

Test Airplane. The test airplane was a North American NAVION, which is an all metal, four place, low wing, single engine airplane. The NAVION is equipped with a Continental E-185 engine, rated at 185 HP at 2300 RPM and 29 inches manifold pressure, at sea level. The wing is unswept, and the tail configuration conventional. The control surfaces are all of beaded skin construction, and have no trailing edge extensions. Aileron and rudder trim tabs are of the fixed bend type. The elevator tab is of conventional design, and can be adjusted from the cockpit.

The test airplane was modified by the removal of the two rear cockpit seats to provide space for the test instrumentation. (Fig. 6). The test airplane had a take-off gross weight of 2870 pounds with full service, pilot and co-pilot, and all test equipment.

A three view drawing and photograph of the NAVION are shown as Fig. 1 and Fig. 2, and the general specifications of the test airplane are tabulated in Table II.

Power Supply. Power available for instrumentation in the test airplane included both 12 and 28 volt direct current, supplied by a 28 volt engine driven generator, and two 12 volt batteries connected in

series. A 500 volt-ampere inverter, with both frequency and voltage regulation, was installed behind the co-pilot's seat to provide 115 volt 400 cycle three phase alternating current power to the rate gyros and the telemeter transmitter.

Considerable effort was expended in obtaining an inverter which could be frequency controlled, since the accuracy of the rate gyros was dependent upon the input frequency being the same as the calibration frequency of 400 cycles per second.

A circuit diagram of the aircraft 28 volt system and the inverter system is included in Fig. 3.

Aircraft Instrumentation. Standard aircraft instruments were used to determine indicated airspeed and altitude. Measurement of the following quantities was required with respect to stability axes: sideslip angle, yaw rate, roll rate, and aileron and rudder position angles. In choosing the type of components needed to measure the above quantities, an attempt was made to utilize instrumentation compatible with the telemetering equipment. For this reason, the transducers selected were of the potentiometer type, not only because they were capable of providing signals of a sufficient magnitude, but also because their excitation source readily provided zero and full scale reference voltages.

In view of some past history in this type of flight testing of various amounts of coupling between the response of the aircraft and certain of the instrumentation components, considerable attention was given to the

choice of transducers with satisfactory frequency and phase response characteristics. These remarks particularly apply to the choice of a suitable device for recording sideslip angle.

In this investigation, sideslip angle was sensed by a light vane mounted on a boom approximately one maximum fuselage diameter (four feet) ahead of the left wing tip. The moment of inertia of the vane was very low, and no gearing was introduced in the linkage in order to keep the natural frequency and damping within acceptable limits. An Electro-Mechanical Laboratory ultra-low torque potentiometer, of only .008 inch-ounces friction torque, was obtained for use with this sideslip vane. In Appendix A is presented a detailed analysis of both the theoretical and experimentally obtained natural frequency and damping ratio of the sideslip vane.

The sideslip vane had originally been designed to operate through an autosyn transmitter, and thus required some modification in order to accommodate a potentiometer.

In order to reduce boom resonance, as had been experience in previous tests with the NAVION, the boom for the sideslip vane was stiffened by three angle strips equally spaced around the periphery, and running the full length of the boom. The sideslip vane and boom are shown in the assembled condition in Fig. 4.

Rudder and aileron angles were measured by 10,000 ohm Model 5301 single turn Helipot precision potentiometers. The rudder pot

was attached to the rudder itself, and was actuated by a cable under spring tension. At the time the instrumentation system was designed, the flight test program was planned to include control inputs from the rudder only. For this reason, the instrumentation installed for recording aileron angle was intended only to indicate if the ailerons remained locked throughout the rudder input and the resulting transient oscillation. Accordingly, the pickoff of aileron angle was made from control cable movement, with the pot attached close to the right aileron in order to avoid the effects of cable stretch. As is discussed in Appendix C, the later decision to include aileron deflections as forcing functions required subsequent correction of the recorded aileron data.

The measurement of yaw and roll rates was made by type 36128 Giannini rate gyros. This type of gyro operates on a power supply of 115 volts 400 cycle three phase AC to the motor, and 115 volt single phase AC to the heater. The transducer is of the potentiometer type, with a DC resistance of 5250 ohms. The gyros were installed as near the aircraft center of gravity as possible. However, since the gyros were of the angular velocity rather than acceleration type, there was not the necessity for precise location that is associated with the latter type gyro. A level and inclinometer were used to align the gyros so that the input axes would be parallel to the appropriate body axis of the aircraft. Since deflection of the gyro spring-restrained gimbal was

only two degrees at full range, cross-coupling effects were considered to be negligible. However, in order to minimize any error due to rate coupling, the spin axis of each gyro was aligned parallel to the body Y-axis. The gyros were bolted directly to a rigid fuselage member. Since the engine vibration frequency was sufficiently above the natural frequency of the gyros (17 cycles per second), there was no engine noise introduced into the gyro signal. These gyros were obtained on loan from the Instrumentation Laboratory of the U. S. Naval Air Test Center, NAS Patuxent River, Maryland.

Signal Circuit Design. The component of the instrumentation which controlled the design of the signal circuit was the sideslip vane. The requirements for recording the sideslip angle without introducing phase differences were negligible torque, and a relatively high natural frequency of the vane. The transducer selected has been shown to have met these specifications (Appendix A), but the fact that it was a 360 degree single turn potentiometer pickup, whereas the sideslip vane was expected to operate through only a moderate arc, necessitated the use of 45 volt DC excitation of the sideslip pot rather than the zero to five volts range supplied to the remaining transducers. Since the resolution of the particular sideslip pot used was exceptionally good, the accuracy of the sideslip system was comparable to that of a system utilizing autosyn pickups, but had none of the problems of AC signal circuits and was completely compatible with the telemetering and recording

equipment. The use of a 45 volt DC signal circuit supply, however, necessitated a method of supplying this voltage to the sideslip circuit, and at the same time, limiting the full scale voltage in the remaining signal circuits to five volts.

In achieving the above, it was desirable to utilize a common DC voltage source for all transducer pickups, since the telemeter was to sample the particular supply voltage available 20 times per second, and correct this to full scale by a continuous calibration.

In addition to the above requirements on the signal circuit design, it was found necessary to bias the sideslip voltage pot in order that the sideslip signal voltage would also vary between zero and a full scale value of approximately five volts.

The particular signal circuit design employed is shown in Fig. 5, in schematic form. The essential element of the circuit is the bias supply voltage potentiometer, pot "A". With the sideslip vane against the limit stop in one direction, pot "A" was adjusted so that the output voltage of the sideslip pot was zero. The vane was then deflected to the opposite limit stop, and the output sideslip pot voltage recorded. Pot "B" was then adjusted to bring the full scale reference voltage, and thus also the voltage in the remaining signal circuits, in agreement with the full scale sideslip voltage. This procedure was repeated two or three times, as necessary, in order to nullify any loading on the system. Once adjusted, however, pots "A" and "B" were locked, and required no further adjustment for the remainder of the project.

During the initial flight and transmission tests, considerable AC ripple was found to enter the DC signal voltage circuits, very likely from the 400 cycle inverter. Condensers C and D in Fig. 5 were installed, and were found to reduce the ripple to a negligible value without otherwise altering the form or amplitude of the signals.

Fig. 6 shows the general location and arrangement of the airborne instrumentation components.

Telemeter System. The telemeter unit was of the pulse width type, and was designed and built by the Applied Science Corporation of Princeton (ASCOP). This unit was the key element in the instrumenta- of this project. The basic functional components of this pulse width system are transducers, all of the potentiometer type; a time division multiplexer, or commutator; and electronic coder, or keyer to put the intelligence into pulse form; an RF transmitter; and ground station equipment for receiving, decoding, and recording the data in usable form.

The airborne component of the system is designated the ASCOP D Series PW Multicoder, and the ground station equipment the ASCOP M Series PW Ground Station. A schematic diagram of the functions of the pulse width data system, as adapted for use with this particular project, is presented in Fig. 7.

A unique feature and very great advantage of pulse width data systems is that due to the multiplexing or time sharing operation, all data

channels traverse the same path during transmission. Since zero and full scale references are transmitted with the data, this results in a calibration signal, effective for all channels, being transmitted 20 times each second. These signals supply a continuous two-point calibration, and thus allow for the removal of almost all of the system errors, with the exception of errors introduced in the instrument pickups and the mechanical switch, and they make possible the use of this telemeter in tests of long duration and varying environmental conditions.

The output voltages from the aircraft instrumentation pickups, and the calibration voltages described above, are sampled in sequence by a rotary switch. At the normal sampling rate of 20 samples per second on each of the 45 channels, the data pulse length for any one channel is short in comparison to the interval from sample to sample. This permits the use of a storage circuit to create a nearly continuous voltage output. The output of the sampling switch is a series of data pulses whose voltage amplitude is proportional to the amplitude of the physical quantity measured by the corresponding pickup. These samples are supplied to an electronic coder circuit (keyer) which converts the amplitude pulses into pulses having time durations proportional to the measured quantities. These pulses are used to produce modulation of the transmitted RF carrier. The RF signal is detected at the ground station, with the output of the receiver being a train of pulses identical in nature to the output of the converter in the airborne equipment.

These pulses are separated by a switch running synchronously with the switch at the transmitter, with the pulses representing individual data channels being placed on separate outputs. The pulses are then demodulated to yield continuous voltages representing the intelligence transmitted.

Ground Station Instrumentation

The ground station equipment included the Telemeter Ground Station (described above), a Magnetic Tape Recorder, a GEDA Analog Computer, and suitable recorders. These components are illustrated in Fig. 8.

Magnetic Tape Recorder. An Ampex Model 309C dual track three speed tape recorder was an integral component of the ground station equipment, and provided a convenient means for recording, storage, and playback of the standard pulse width modulated data. Provisions were also included for placing voice transmissions directly on the magnetic tape from either or both the aircraft and the ground station.

GEDA Analog Computer. The analog computer used in this investigation was a Goodyear Aircraft Corporation Model L3 (GEDA) linear electronic differential analyzer. Twenty-four automatically stabilized DC computing amplifiers were available with open-loop DC gain of greater than 5×10^7, and negligible drift. The computer

incorporated an automatic error indicator, and had a guaranteed accuracy of one percent. Provisions were available for accurately setting computer board potentiometers by the use of a special null indicator.

Data Recorder. Qualitative analysis of the flight data during tape playbacks was made on a Brush two channel recorder. Once the particular data run was selected for further analysis, a Sanborn Model 154-100B four channel recorder was used. This instrument had a very high natural frequency (42 cps), and the low frequency response was flat to zero cps.

Instrument Calibration

Five components of the instrumentation system required calibration. These were the two rate gyros, the two control deflection potentiometers, and the sideslip vane potentiometer. The aircraft altitude and airspeed indicating systems were not calibrated, as previous calibrations indicated that the errors in these systems were negligible for the conditions of this investigation.

The two rate gyros were calibrated on a pendulum which consisted of a 3/4 inch diameter aluminum shaft and a 12 inch diameter instrument pan. The pendulum, the overall length of which was 121.75 inches, was pinned to the overhead truss structure of the Forrestal hangar. A scale was mounted on a small table in such a way that displacement

of the pan from its rest position could be measured. The gyros were mounted one at a time on a wooden base plate which was clamped to the pendulum pan, and their potentiometer outputs were connected to a Brush Pen Recorder. The pendulum was displaced from its rest position and allowed to swing freely. Because of friction in the system, swing amplitudes were measured on two successive swings in the same direction and averaged. The two maximum voltages recorded during the swing were also averaged and the maximum rate attained during the swing was determined from the following relation:

$$\dot{\Theta}_{max} = \frac{d}{\ell} \frac{360}{P}$$

where:

P = natural period of the pendulum, determined from the Brush Recorder trace, seconds.

ℓ = length of the pendulum, inches.

d = average maximum displacement of the pan from rest position, inches.

The pendulum was allowed to swing until once again at rest with readings taken as described above over the entire range of gyro rates. The angular rate gradient of both gyros was found to be linear and equal to 0.610 degrees per second, per percent full scale potentiometer voltage. The gyro calibration curves are presented as Fig. 9. It was found that the gyros were very sensitive to the frequency of the 400

cycle supply voltage and as a result, great care was taken during calibration, and also during the actual flight test program, to maintain the frequency of the supply voltage at exactly 400 cycles per second.

The control deflection potentiometers were calibrated by measuring the resistance between the output terminals over the full range of control deflections. The actual control deflections were measured with a vernier protractor capable of accuracy to 0.1 degree. The rudder deflection gradient was found to be linear and equal to 0.405 degrees per percent full scale potentiometer voltage. The aileron pot calibration was based on total aileron angle, and was performed over the entire range of aileron travel in order to determine the extent of aileron differential for the NAVION aircraft. The calibration was then converted to average aileron angle, and was found to be linear at a constant value of 0.1933 degrees per percent full scale, throughout the deflection range used in the flight test, which included -10 to 10 degrees. The amount of aileron differential gearing in this range was found to be extremely small.

The sideslip vane potentiometer was calibrated in the same manner as the control deflection potentiometers, and the calibration curve is presented in Fig. 10. The sideslip gradient was found to be linear and equal to 0.468 degrees per persent full scale potentiometer voltage.

Since the telemeter equipment corrected its output to percent full scale voltage and since full scale voltage on all the signal circuit potentiometers varied by the same increment as the reference voltage for small fluctuations of the reference, it was unnecessary to calibrate the potentiometers through the telemeter equipment.

Careful consideration was given to the possible errors which might be introduced in the data by the dynamics of the recording instruments. The natural frequency of the rate gyros was 17 cycles per second and their damping ratio was between .45 and .7. The natural frequency and damping ratio for the sideslip vane were experimentally determined in flight to be 15.44 cps and .081 respectively. (See Appendix A.) Since the natural frequency of the aircraft was approximately 0.4 cycles per second, the attenuation of the signals due to the dynamics of the instruments was effectively zero.

PROCEDURE

General

Aircraft transient responses in the lateral modes of motion were obtained by introducing rudder and aileron control motions of the pulse, doublet, and step-function types. Rudder pulses, rudder doublets, and aileron doublets were found to be the most effective in exciting the "Dutch Roll" motion, which in turn produced the most satisfactory transient time histories for the investigation in question. Aileron step-functions were also used, however, primarily to provide the time history of roll-rate response to lateral control motion.

Ideally, sufficient transient response data for all types of forcing functions could be obtained in one flight of approximately an hour's duration. However, due primarily to the need of the investigators to gain some proficiency with the instrumentation and technique of applying satisfactory forcing functions, several flights were made in the process of collecting data. It is worthy of note that the basic scheme of instrumentation and data collection proved singularly reliable during the flight test - data collection phase. After initial installation the instrumentation required only a very minimum of modification and adjustment, and in each instance the trouble was minor in nature and easily remedied.

Aircraft

Preflight preparation consisted of checking the full scale voltage applied to the sideslip potentiometer to insure that it matched that of the other signal potentiometers, and to insure that the full scale signal voltage did not exceed the 4 - 6 volt range which the telemetering equipment needed for automatic scale calibration. The fuel tank was checked and if necessary topped-off to insure that the aircraft weight at the beginning of each flight was constant. When deemed advisable, a complete ground check of all communication and signal transmission circuits was made prior to take-off. After completing the ground checks all test equipment and the aircraft generator were secured to insure maximum engine power for take-off.

During the climb to test altitude, the generator and inverter were energized and power was applied to the rate gyro heaters and to the airborne telemeter heater and filament circuits. Upon reaching test altitude, voice contact was established with the telemeter ground station and all instrumentation circuits were energized. Because of an apparent deficiency in the inverter frequency control, the inverter frequency was monitored continuously and maintained at 400 cps by varying the DC voltage supplied by the aircraft generator to the inverter. Voltage control was obtained by means of an instrument-panel mounted potentiometer which was tied into the aircraft voltage regulator circuit (Operation of the synchronous motors in the rate gyros at exactly 400 cps was

necessary to insure that the output signals followed the calibration curves obtained at that frequency).

All flight tests were conducted at a density altitude of 5000 feet and at a true airspeed of 129.2 mph (120 mph IAS at 5000 density altitude). A large plot of free air temperature versus pressure altitude was carried in the cockpit to facilitate adjusting pressure altitude (altimeter set at 29.92 in. Hg) with temperature to obtain and maintain 5000 feet density altitude.

The general technique employed in the actual test runs fits the following description. A condition of steady-state flight was established at test altitude and airspeed and held for at least 30 seconds prior to each control input. This period of steady-state flight insured that the aircraft was as nearly trimmed and established in steady state conditions as possible, and provided a sufficient period of recorded steady state signals to allow for circuit zero-signal biasing when the data was played back into the analog computer or pen recorder. At the end of the steady state period a radio transmission identifying the type of control displacement to be made was sent and recorded on the magnetic tape. Simultaneously, all controls were locked mechanically in the cockpit with the exception of the control to be displaced. Five seconds after the above transmission the control forcing function was applied and the control was then returned to the original steady-state position and locked. All controls were held locked until the resulting aircraft

oscillation had essentially subsided. In the case of the aileron step functions the displacement was applied as rapidly as possible and the control was then held as rigidly as possible. The resulting motion in this case was permitted to proceed for 4 to 6 seconds before recovery was initiated.

To lock the elevator and ailerons when forcing the aircraft with rudder displacements, a chain and turnbuckle system attached to the deck on the right side of the cockpit was used. The copilot's control wheel was removed and replaced by a sprocket wheel with a set screw to lock it to the control shaft. When the aircraft was established in steady-state flight, the sprocket wheel was pushed forward on the control shaft until it butted against the instrument panel. The chain was then put on the sprocket and the turnbuckles taken up, making the chain taut. Just prior to initiating the rudder deflection, the set screw was tightened, locking the sprocket fitting to the control shaft. With the chain on and tight, the ailerons were effectively locked, and, with the sprocket fitting against the instrument panel, no forward motion of the control shaft was possible. The copilot then held forward pressure on the sprocket fitting to prevent aft movement of the control shaft.

To lock the rudder when putting in aileron displacements, and to return the rudder to its steady-state position after rudder displacements, a chain and turnbuckle system on the pilot's right rudder pedal was employed. This was attached to the right hand seat track on the

pilot's side. Because the aircraft required a slight amount of left rudder for trim at the test flight condition, this attachment was also useful in establishing trimmed flight by adjusting the turnbuckle.

Ground Station

In order to visually monitor the data runs, an external patchboard provided on the telemeter receiver (See Fig. 8) was wired in such a way as to utilize a voltmeter-type translator for each of the recorded variables, and also to allow the decoded output to be placed on a pen recorder. The telemeter receiver and the magnetic tape recorder had been integrated prior to this investigation, thus requiring only the proper positioning of controls on the telemeter console to accomplish tape recording of the flight data. Each quantity measured during the flight tests was transmitted on three separate telemeter channels. Thus, each measured variable was sampled 60 times each second. Once the airborne equipment was operating, the telemeter receiver was tuned for maximum signal reception, and the "zero" and "full-scale" reference voltages were adjusted for proper calibration of output signals.

All pertinent communications between the ground station and the aircraft were recorded on magnetic tape along with the flight test data. Prior to commencing the recording of test data on each flight, the ground station operator pre-recorded on the magnetic tape the data necessary to identify the particular flight, and test conditions as

regarded aircraft weight, lift coefficient, and the telemeter channels being used for each measured quantity.

Concurrent with the reception and tape recording of the flight test data, a two or four channel pen recorder was used to present visually for monitoring all or a part of the test data as the maneuvers were being performed. Thus, if the control input did not produce well excited responses, or if a control surface that was to be held locked moved inadvertently, or if the forcing control was not returned to, and held at, the original steady-state position this was immediately apparent. In any of these eventualities the run could be rejected immediately on a qualitative basis and the test repeated.

Data Reduction

The only flight variable requiring correction to the measured quantity was sideslip angle (β) which had to be corrected for location of the sideslip vane ahead of the aircraft center of gravity. The required correction was:

$$\beta_{\text{corr.}} = \beta_{\text{measured}} - \frac{l_{sv}}{V}(\dot{\psi})$$

In order to have all flight variable signals in the same angle-time-voltage relationship, the flight data was processed through scaling circuits on the analog computer prior to plotting on a pen recorder. The scaling factors used were determined from the calibration curves for each of the signal potentiometers. Where necessary, the signs of

the measured variables were changed to correspond to the sign of the corresponding output of the analog probelm. A .25 uf capacitor was placed across each of the output terminals of the telemeter. This size capacitor was found to help in eliminating high frequency noise in the flight data signals while at the same time having negligible effect on the amplitude and phase of the signals. The computer circuits used in correcting the sideslip angle and scaling the flight test data were as follows:

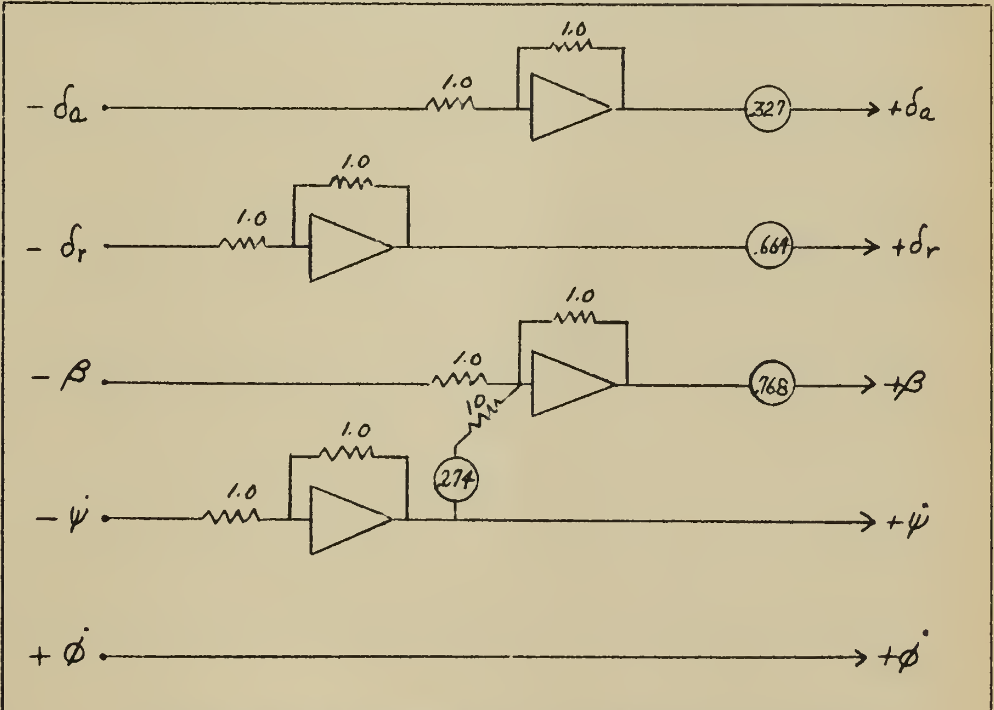

Flight Data Scaling and Correction Circuits

In order to use the actual flight test control deflections as forcing functions for the analog problem it was necessary to feed them into the computer through a bias circuit so that the steady-state control position signals, which were of the order of -50 volts at the telemeter output

terminals, could be reduced to a zero voltage input to the analog problem. A potentiometer was also required in each input circuit to adjust the amplitude of the control deflection voltage to match the scaled magnitude of the control deflection on the flight test data plots. As in the data reduction circuits, a .25 uf capacitor was put across the telemeter output terminals. The above described circuits are included in Fig. 13.

DISCUSSION

General Description of Overall Program

In obtaining flight data, four different types of control deflections were used to excite the lateral modes of the NAVION. These were a rudder pulse, a rudder doublet, an aileron doublet, and an aileron step function. By means of telemeter equipment, the transient response of the aircraft as well as the control deflections as a function of time were recorded on magnetic tape at the ground station. From a large selection of such data, one representative trace was made of each of the four types of forcing functions mentioned above. This was accomplished by processing the flight data through scaling circuits in the analog computer and recording the variables in time history form on a Sanborn recorder. A transparent overlay was then made of each of the four traces of scaled flight data in order to facilitate comparison of the flight and computer responses.

Next, the lateral stability derivatives of the NAVION were theoretically estimated. The lateral equations of motion based on these derivatives were placed on an analog computer in such a way as to enable independent variation of each stability derivative. The magnetically recorded signal corresponding to one of the four chosen control deflections was then fed directly into the computer to force the analog. Both the character and magnitude of the forcing function signal were checked

by means of the overlay of the flight data. Once the forcing function was properly adjusted, the computer responses to the forcing function were recorded and compared to the flight responses by means of the same overlay. Adjustments were then made to the computer derivatives as necessary to improve the match between the flight data and the computer response. The procedure of forcing the computer was then repeated, using another one of the four forcing signals, and making appropriate adjustments to derivative values. This procedure proved to be a converging iteration process when repeated several times, using all four types of forcing functions. When a set of derivatives was found such that the response of the computer gave satisfactory matching with the flight data for all four of the forcing functions, and no further improvement seemed justifiable in relation to the amount of time involved, the value of each stability derivative was read out of the computer and tabulated.

Preliminary Considerations

Theoretical Background.

At the onset, of the investigation, it was necessary to make a purely theoretical analysis of the proposed method of attack of the problem. In effect, the pertinent questions were:

a) If a set of coefficients is determined which, when placed in the equations of motion, duplicate the response of the aircraft, can it be proved that these coefficients are unique rather than just one set of an entire family of possible solutions?

b) With two possible methods of exciting the lateral mode, i.e., the rudder and the ailerons, how much data should be collected and what should be the character of the control deflections used to excite the motion?

Examining these questions, it was determined that one was related to the other. The answer to question (a) is a function of the amount of independent data available. Should there be a case where, in fact, an entire family of solutions exists, then there would be an interdependence between at least two of the coefficients, and one coefficient could be expressed in terms of one or more of the other coefficients. If it were then possible to obtain more independent data, a point would be reached where there were sufficient conditions to limit the family of solutions to a single solution. Applying the latter case to the investigation at hand, it would then be known that if a set of coefficients were obtained by the response-matching technique, these coefficients would be unique, i.e., the only set of coefficients which would produce the matching of responses. The stability derivatives contained in the lumped coefficients would then indeed be the stability derivatives of the aircraft. The amount of independent data available would be in part a function of the control deflections used, and in addition would depend on the number of quantities such as roll rate, yaw rate, and sideslip angle which were recorded during the response.

Fortunately, a theoretical investigation into this subject was

available in Ref. 4. The authors, Messrs. Klein and Sedney, assume that the equations of motion are linear with constant coefficients (however, it is pointed out that the same method of analysis can be applied to more general types of equations), and also that the data is free from experimental error. The results of their analysis is a simple working rule which can be stated in words as follows: In each equation describing a system, the number of unknown coefficients which can be determined plus the number of known coefficients which may be checked are equal to the total number of measured quantities less the number of equations.

This result was applied to the lateral equations of motion of the NAVION, with J_x, J_z, J_{xz}, and C_L known . The quantities which were to be recorded during the testing were roll rate, yaw rate, sideslip angle, and control deflections. In application of the Klein and Sedney criterion, roll angle, roll acceleration, yaw angle, yaw acceleration, and sideslip rate are considered to be recorded in a concealed form in the other time histories, since they are obtainable by differentiation or integration of the appropriate trace. By following the working rule of the criterion, it was found that in each of the three equations of motion there was actually an excess of independent data under the recording conditions proposed, and therefore the solution for the coefficients would be unique.

Practical Aspects. Although no theoretical limitation exists in the case of the lateral mode, there is a practical limitation which applies to the analysis of all dynamic response data. The following statements are extracted from Chapter 10 of Ref. 1:

> Instrument errors and unknown atmospheric disturbances are usually present to a sufficient degree to introduce significant errors into the solution of the inverse problem. As a general qualitative rule, the accuracy with which one can obtain each of the stability derivatives is associated with the importance of that stability derivative in influencing the motion of the aircraft during the test, the highest accuracy being obtained for the more important stability derivatives.
>
> Consideration of the means for improving the accuracy with which the less important derivatives can be obtained leads to these three approaches to the problem:
>
> 1. Overall improvement of the accuracy of the recording instrumentation and improvement of the calibration and pre-flight testing techniques.
>
> 2. Selection of test maneuvers which increase the force and moment contributions due to the smaller derivatives compared to the forces and moments due to the other derivatives.
>
> 3. Performance of flight tests under so-called ideal conditions, i.e., air is smooth and stable.

Selection of flight test instrumentation components was made with the requirements of (1) above in mind. As previously discussed under "Airborne Instrumentation," the transducers were chosen to be compatible with the recording instrumentation in order to eliminate excessive electronic modification of the signal voltages prior to recording. This effectively reduced possible sources of error. Calibration

was carefully performed and the resolution and linearity of the components are readily apparent from the calibration curves, as presented in Fig. 9 and Fig. 10. Test flights were performed under conditions of smooth and stable air.

The selection of suitable forcing functions for the lateral mode was initially considered from the viewpoint of Klein and Sedney, who state that theoretically, the response of the aircraft to a single forcing function is sufficient to establish the stability derivatives, with the exception of the control derivatives. Accordingly, a rudder pulse was selected as the forcing function most suitable for excitation of the lateral mode. However, the prospect of extending the method of analysis to obtain all of the control derivatives, plus the possibility of improving the accuracy of certain derivatives through the use of additional forcing functions, was made very attractive when considered from the standpoint of paragraph (2) of the above quotation from Ref. 1. Four forcing functions were therefore decided upon. Considering the rudder pulse as the basic data, a rudder doublet was utilized to increase the amplitudes of the lateral responses, and to reduce the tendency of the aircraft to fall off on one wing during the transient as had been observed in the case of excitation by a rudder pulse. The aileron doublet was considered as an effective means of evaluating C_{ℓ_p}, C_{n_p}, and the aileron derivatives, whereas a time-history of the roll rate response to an aileron step function was considered to be the best means for analyzing the stability of the spiral mode.

Analog of the Test Aircraft

Theoretical Approximation of Derivatives. In order to construct an analog of the lateral equations of motion, it was necessary to estimate the value of the stability derivatives from whence the approximate value of each lumped coefficient could be determined. Anticipating the possibility of extremely slow convergence of the iteration process used on the computer, the theoretical value for each derivative was determined as accurately as possible by several different methods and then a median value was taken. The results and a complete explanation of this work is contained in Appendix B.

Lateral Equations of Motion. The lateral equations of motion of a linear aircraft are as follows:

$$(C_{Y_\beta} - 2D)\beta - 2D\psi + C_L\phi + C_{Y_{\delta_r}}\delta_r = 0$$

$$\mu C_{\ell_\beta}\beta + \left(\frac{C_{\ell_r}}{2} + J_{xz}D\right)D\psi + \left(\frac{C_{\ell_p}}{2}D - J_x D^2\right)\phi + \mu C_{\ell_{\delta_a}}\delta_a + \mu C_{\ell_{\delta_r}}\delta_r = 0$$

$$\mu C_{n_\beta}\beta + \left(\frac{C_{n_r}}{2} - J_z D\right)D\psi + \left(\frac{C_{n_p}}{2} + J_{xz}D^2\right)\phi + \mu C_{n_{\delta_a}}\delta_a + \mu C_{n_{\delta_r}}\delta_r = 0$$

For ease of construction of the analogy the equations can be rewritten incorporating the following changes:

a) in terms of the highest derivative.

b) in real time by the explicit insertion of the non-dimensional time constant, τ.

c) for simplicity, the algebraic signs changed where necessary so that all work from this point on could be conducted in terms of the absolute value of each derivative.

The resulting equations are:

$$-\dot{\beta} = \frac{|C_{Y\beta}|}{2\tau}\beta + \dot{\psi} - \frac{C_L}{2\tau}\phi - \frac{|C_{Y\delta_r}|}{2\tau}\delta_r$$

$$\ddot{\phi} = -\mu\frac{|C_{l\beta}|}{\tau^2 J_x}\beta - \frac{|C_{l_r}|}{2\tau J_x}\dot{\psi} - \frac{J_{xz}}{\tau J_x}\ddot{\psi} + \frac{|C_{l_p}|}{2\tau J_x}\dot{\phi} + \mu\frac{|C_{l_{\delta_a}}|}{\tau^2 J_x}\delta_a + \mu\frac{|C_{l_{\delta_r}}|}{\tau^2 J_x}\delta_r$$

$$\ddot{\psi} = -\mu\frac{|C_{n\beta}|}{\tau^2 J_z}\beta - \frac{|C_{n_r}|}{2\tau J_z}\dot{\psi} - \frac{|C_{n_p}|}{2\tau J_z}\dot{\phi} + \frac{J_{xz}}{\tau J_z}\ddot{\phi} + \mu\frac{|C_{n_{\delta_a}}|}{\tau^2 J_z}\delta_a + \mu\frac{|C_{n_{\delta_r}}|}{\tau^2 J_z}\delta_r$$

The numerical values of the non-dimensional constants and the estimated derivatives were then substituted into the equations. The terms containing J_{xz} were found to be so small in comparison to the other terms that they were immediately discarded as negligible:

$$-\dot{\beta} = .249\,\beta + \dot{\psi} - .171\,\phi - .0468\,\delta_r$$

$$\ddot{\phi} = -17.8\,\beta + 1.94\,\dot{\psi} - 8.74\,\dot{\phi} + 1.89\,\delta_r + 21.8\,\delta_a$$

$$\ddot{\psi} = 3.99\,\beta - .529\,\dot{\psi} - .289\,\dot{\phi} - 3.65\,\delta_r - .208\,\delta_a$$

The constructed analog for the above equations is shown schematically in Fig. 11.

Development of Method of Analysis

Prior to the analysis of the actual flight test data, a step by step procedure was developed for matching the computer response to flight data. First, an investigation was made to determine the effect of each stability derivative on the response of the system in terms of amplitude, period, and damping. The analog of the test airplane (Fig. 11) was placed on the analog computer, and the potentiometers set to correspond to the NAVION theoretical stability derivatives of Table V. An electronic function generator was used to force the analog with a square pulse type function, to approximate the form of a rudder pulse. A series of runs was then made during which the stability derivatives were varied successively by a factor of two and then returned to their original theoretical values. From these tests, the change in the response due to the change of any one derivative was recorded, and the results included in Table III-a. A cross-table was then prepared showing which derivatives should be varied to obtain a desired change in the response of the system. These results are shown in Table III-b.

With the aid of the information presented in Tables III-a and III-b, an iterative procedure for the matching of computer response with flight data was outlined as follows:

(a) Compare flight data and computer response curves obtained from the same forcing function. Note discrepancies in

amplitude, phase, damping, etc., between corresponding responses.

(b) Concentrate on the major discrepancy. By reference to Tables III-a and III-b, determine which derivative, or derivatives, could be altered to correct this type of discrepancy.

(c) Iteratively apply the corrections indicated in (b) above, commencing with the derivative having the most pronounced effect on the particular discrepancy. When no further improvement can be observed by adjusting the value of the first derivative, continue in a consecutive adjustment of all the derivatives affecting the discrepancy.

(d) Repeat (a), (b), and (c) above for additional discrepancies until general agreement is obtained between flight data and the computer response curves.

(e) Continue by comparing flight data and computer response curves obtained from a second forcing function. Again, repeat (a), (b), and (c) until agreement is obtained.

(f) Repeat (e) for as many forcing functions as are available or practical. When the response to all forcing functions have been examined once, return to the first forcing function and repeat the entire process outlined above; continue until a set of derivatives is obtained which give the best possible response match to all forcing functions used.

Preliminary Test of Feasibility of Method

A program was next performed to establish the feasibility of using an analog computer to curve-fit flight data and yield unique stability derivatives. It was considered that if the transient response of the computer to a rudder-pulse type of forcing function were recorded, and considered as error-free "flight data," and the computer potentiometers corresponding to stability derivatives then changed, that subsequent re-matching of the original synthetic "flight data" response should yield computer potentiometer settings identical to those of the "flight data." It was found that this type of analysis produced excellent results, with the exception of the determination of C_{l_r} , C_{y_β} , and $C_{y_{\delta_r}}$. The responses were found to be too insensitive to changes in these three derivatives in order to establish them with satisfactory accuracy. The final value of C_{n_p} contained an error of approximately ten percent. All other derivatives were obtained within an error of five percent. C_{n_β} and C_{l_β} were obtained with virtually no error ; this latter result was anticipated, from consideration of the large relative magnitude of the lumped coefficients containing these terms.

Unfortunately, the above program was not extended to the use of an aileron input. Although the results were gratifying for the rudder forcing function used, they might well have been improved if the additional forcing function data had been utilized. In particular, the use of

aileron forcing functions might have resulted in a better indication of the effect of the derivative C_{n_p}.

The investigators considered that the results of this preliminary program established the feasibility of the basic method. It was also encouraging to note that with a minimum of practice, the iteration procedure developed for matching the analog responses to flight data resulted in moderately rapid convergence. With ten stability derivatives all acting as variables in the inverse problem, a great deal of difficulty had been anticipated in effecting a convergence when using what is basically a simple iteration process, but to the degree of accuracy obtained in the results mentioned above, no significant problems were realized.

In future applications of this method, the procedures described in the sections "Development of Method of Analysis" and "Preliminary Test of Feasibility of Method" would be useful to an investigator from two standpoints: they would provide data on the sensitivity of the specific configuration under investigation to changes in individual derivatives, and would provide valuable experience in manipulating the coefficients to obtain the desired response.

Application of Method to Flight Test Data

The four control deflections which were selected and the corresponding responses of the aircraft in the three variables β, $\dot{\psi}$, and $\dot{\phi}$ are shown in Figs. 15 - 18. As mentioned previously, a transparent

overlay was made of each of these four sets of data to facilitate comparison of the computer response with the flight data.

One of the important features of the instrumentation was the fact that signals proportional to the four control deflections were available for forcing the computer by playing the recording of flight data, stored on the magnetic tape, through the decoding component of the telemeter ground station. From the output of the telemeter, the circuity shown in Fig. 13 was used to bias the steady state signals of the controls to zero and to provide proper scaling of the control deflection signal magnitudes. Without this feature, it would have been necessary to obtain the forcing function for the computer from an electronic function generator, with limited prospects for exact duplication of the aircraft control deflections. The use of the exact forcing function from the flight data thus eliminated a possible source of error by maximizing the compatibility of the data collection system and the analog computer.

The relationship between the actual aircraft response and the response of the analog containing the initial theoretical derivatives, when each was forced by a rudder pulse, is shown in Fig. 14. With this initial analog response (Fig. 14) as a starting point, the attempt to curve-fit the analog to the flight data was commenced.

The initial steps of the curve fitting process were the same as the first four parts of the procedure previously described in "Development of Method of Analysis." Reference to Fig. 14 indicated that the most

obvious discrepancy was in the period of the Dutch roll oscillation. Since Tables III-a and III-b showed C_{n_β} to be the derivative most effective in adjusting the period, the value of C_{n_β} was increased by small increments until a relatively good period match was obtained. The values of the rudder control derivatives ($C_{n_{\delta_r}}$, $C_{y_{\delta_r}}$, $C_{l_{\delta_r}}$) were then corrected to reflect the change in C_{n_β}. The next steps were to attack successively the discrepancies in damping, yaw-rate amplitude, and roll-rate amplitude by adjusting the appropriate derivatives in accordance with the information in Tables III-a and III-b. This procedure improved the match between the analog and the aircraft responses appreciably. However, in an attempt to further improve the matching, and at the same time gain further insight into the interplay of the effects of the various derivatives, all derivatives not adjusted in the foregoing procedures were successively altered to observe their effect on the analog responses. When no change, or an adverse change, in the responses was encountered, the derivative under investigation was returned to its original value. Those changes which appeared beneficial were retained. In each case, the effect of altering a derivative, and the extent of the change were recorded.

After a reasonably close match between the analog and aircraft responses to a rudder pulse was obtained, the analog was next forced by a rudder doublet, with the computer potentiometers still set on the derivatives established by matching responses to the rudder pulse.

The procedure which was then followed to minimize the discrepancies between the analog and aircraft responses was identical to that used for response to a rudder pulse, and again produced an improvement in the analog responses.

The responses to an aileron doublet and aileron step function were then investigated in a like manner; that is, by first concentrating on the derivative changes indicated in Tables III-a and III-b, and then investigating the individual effects of all other derivatives. During the initial analysis of the aileron data, it was determined that an error existed in the aileron signal due to cable stretch in the control system. Corrections required for this error are discussed in Appendix C.

During the conduct of the actual flight tests, it had been noted that in response to an aileron step function, the aircraft developed a nose-down attitude within two seconds after the application of the aileron displacement. This was caused by the large roll angle that developed. The resulting errors in the β and $\dot{\psi}$ traces were readily apparent and consequently, these two variables were disregarded in this case. The only matching that was attempted with aileron step forcing functions were the amplitude of the initial peak of the roll rate response, and the neutral stability of the spiral mode as indicated by the constant mean value of roll rate after the roll rate response had reached its initial peak value. The rapid development of the nose-down attitude when the aircraft was forced by an aileron step function could

have been avoided by the use of an initial condition, such as a steady sideslip. This would have extended the time during which the airplane was in the linear approximation range. Since the equations of motion of the analog are developed for perturbations from steady state, a similar initial condition would not be required when forcing the computer.

After completion of one series of iterations for the values of the stability derivatives, the procedure was repeated for all forcing functions, again starting with the rudder pulse. It was noted that good matching was quickly obtained for any one of the forcing functions taken individually, but a shift to the other forcing functions offered a relatively poor match in the early stages. Gradually, however, as a result of the experience obtained, and by reference to the records of the effects of varying the individual derivatives, new procedures for establishing the value of some of the derivatives became apparent. These procedures represented a more definite method of evaluating the corresponding derivatives than did the influences indicated in Tables III-a and III-b, because in each case a particular response characteristic was controlled by an individual derivative. The derivatives and their individual effects are as follows:

C_{n_β} - The period of the Dutch roll mode is controlled by this derivative. This derivative has more than ten times the effect on the period than does any of the other derivatives.

C_{n_r} - C_{n_r} has a controlling effect on the damping of the Dutch roll mode when the analog is forced by a rudder deflection.

$C_{n_{\delta_r}}$ - Changing this derivative changes the effectiveness of the rudder in producing yaw. Therefore, $C_{n_{\delta_r}}$ can be established by matching β and $\dot{\psi}$ amplitudes due to a rudder deflection.

C_{l_β} - The magnitude of this derivative controls the matching of $\dot{\phi}$ response in two respects; phase and amplitude. Phase error in the initial $\dot{\phi}$ response of the analog is affected considerably by this derivative.

$C_{l_{\delta_a}}$ - When the airplane is forced with an aileron step function, the Dutch roll mode is excited to such a small degree that the initial peak of the $\dot{\phi}$ response can be attributed to the rolling mode and the magnitude of $C_{l_{\delta_a}}$. For a given C_{l_p} , $C_{l_{\delta_a}}$ can be determined by matching the initial peak of the $\dot{\phi}$ response. Determination of the precise value of C_{l_p} is explained below.

C_{l_p} Just as C_{n_r} controls the damping of the Dutch roll mode, C_{l_p} controls the damping of the rolling mode. With $C_{l_{\delta_a}}$ adjusted as described above, C_{l_p} can be determined by matching the $\dot{\phi}$ response to an

aileron doublet, especially during the latter half of the aileron input.

$C_{l_{\delta_r}}$ - The effect of this derivative is readily apparent in the $\dot{\phi}$ response as an initial adverse $\dot{\phi}$ due to a rudder deflection. Matching the initial form of the $\dot{\phi}$ response will thus establish $C_{l_{\delta_r}}$.

$\left.\begin{matrix} C_{n_p} \\ C_{n_{\delta_a}} \end{matrix}\right)$ - In the response of the computer analog to a rudder deflection, C_{n_p} has only a small effect. However, an upper and lower limit can be established for C_{n_p}, beyond which the character of the $\dot{\psi}$ trace is noticeably altered in magnitude. In the case of an aileron deflection, the effects of C_{n_p} and $C_{n_{\delta_a}}$ are so similar that one can be replaced by the other to a large extent. If an iteration is performed between these two derivatives, however, maintaining C_{n_p} within the limits developed during a rudder deflection, until the best match is obtained in $\dot{\psi}$ due to an aileron doublet, C_{n_p} and $C_{n_{\delta_a}}$ can be determined within reasonable limits of accuracy.

C_{l_r} - Only a very rough value of this derivative can be established. Gross changes in C_{l_r} will effect the stability of the spiral mode. The $\dot{\phi}$ response to an aileron step function is an indication of the spiral

mode stability: a constant mean value of $\dot{\phi}$ indicates neutral stability, a decreasing mean value indicates positive stability and an increasing mean value indicates negative stability of the spiral mode. Since the other three derivatives which affect the spiral mode (C_{n_β} , C_{n_r} , C_{l_β}) can be determined by the methods outlined above, the value of C_{l_r} can be adjusted to match the character of the mean response to an aileron step function.

$C_{y_{\delta_r}}$)
C_{y_β}) - Because of the insensitivity of the responses to changes in these derivatives, no refinement of the theoretically determined values was possible.

The above relations are summarized in Table IV.

By the time sufficient information had been accumulated to develop the procedures outlined above, the initial discrepancies between the analog and the aircraft responses, for all four forcing functions, had been appreciably reduced. Subsequent use of the iteration procedure, in the case of each forcing function and its related responses, was confined primarily to adjustments in the derivatives which were based on the relationships of Table IV. In addition, when working with the responses to the rudder forcing functions, care was taken not to make large changes in those derivatives which had been established primarily

by matching responses to aileron forcing functions. This restriction was found necessary, since alteration of the aforementioned derivatives generally resulted in only minor improvements in the rudder cases, but had an appreciable adverse affect on the matching of the responses in the aileron cases. The same restriction was applied when matching responses to aileron forcing functions; in this case, no extensive changes were made in those derivatives which had been established primarily by matching responses to rudder forcing functions.

When a set of derivatives was found such that the responses of the computer gave satisfactory matching with the flight data for all four of the forcing functions, and no further improvement seemed justifiable in relation to the amount of time it would involve, the final value of each derivative was read off of the computer potentiometers and recorded.

RESULTS

The final values of the lateral stability derivatives of the NAVION as determined by the method of this report are tabulated and compared with the initial theoretical values in Table V. The matching of the responses of the final computer configuration to the flight test data for all four types of forcing functions are presented in Figs. 15 - 18.

During the iteration process, a better match had been obtained to the responses for each of the four forcing functions taken individually, but no single set of derivatives gave as good a match to the responses of all four forcing functions taken as a group as did the final set of derivatives listed in Table V. The major discrepancies remaining in the final matches are the generally low response of the analog in the β variable for all forcing functions ; the too large amplitude response in the $\dot{\psi}$ variable for rudder doublet forcing functions ; and the initial $\dot{\psi}$ response to the aileron doublet. It is felt that had more time been available, further investigation into the interrelated effects of the cross derivatives C_{n_p} and C_{l_r} would have resulted in nearly perfect response matches in the $\dot{\psi}$ and ϕ' variables when using the rudder forcing functions.

The accuracy of the final value of each derivative is directly related to the sensitivity of the system response to changes in the derivative. The derivatives $C_{l_{\delta_a}}$, $C_{l_{\delta_r}}$, C_{n_β} , $C_{n_{\delta_r}}$, C_{l_β} ,

C_{l_p} , and C_{n_r} are judged to be very accurately determined by the method. (See Appendix C concerning the accuracy of the specific values for $C_{l_{\delta_a}}$ and $C_{n_{\delta_a}}$ of this report.) The values for C_{l_r}, C_{n_p}, and $C_{n_{\delta_a}}$ are susceptible to somewhat larger error due to the smaller effects they produce on the response, and also due to overlapping effects in the case of C_{n_p} and $C_{n_{\delta_a}}$. Finally, the value of the derivatives C_{y_β} and $C_{y_{\delta_r}}$ could not be established with satisfactory accuracy. Other types of flight maneuvers might be advantageous in establishing these latter derivatives.

The proposed method of extracting stability derivatives from transient flight data was determined to be completely feasible. As mentioned previously, there are inherent difficulties in the process of extracting all of the derivatives from flight data regardless of the method used. For certain applications, however, no better criterion could be established for obtaining the values of the stability derivatives than to match the response of the analog containing these derivatives to the response of the actual aircraft. In the field of servomechanisms, for example, this criterion would be considered to be of prime importance.

Another advantage of the method would be its economy in time, both in obtaining flight data and in extracting the derivatives from that data. In obtaining the flight data, any arbitrary forcing function can be used, providing it offers sufficient excitation of the modes of aircraft motion. Use of the telemeter data collection system permitted

convenient monitoring of flight data during the flights, and thus when necessary, instructions could be given to the pilot, to improve the responses obtained. Normally this would allow the recording of all the data for one flight condition in a matter of minutes. The ease of extracting the derivatives would tend to increase with practice. Undoubtedly, Table IV, which contains procedures for establishing several of the derivatives, could be expanded with the aid of more time and experience with the method. For this reason, it is felt that better matching than is illustrated in this report would definitely be possible. It is important to note that the results of this investigation were obtained for the aircraft in the cruise condition only. Because of the large variation of certain stability derivatives with changes in flight conditions, further investigation of the method throughout a range of flight conditions is recommended. There is virtually no chance of computational errors affecting the results, for once the analog has been completed the computations are performed by the computer.

Although the theoretical estimates of the derivatives were made as accurately as possible in this investigation, it was found that the rate of convergence of the iteration process was sufficiently rapid in the first stages to suggest that very rough estimates of the derivative values would be sufficient for use as initial computer settings. The time involved in refining the rough estimates would more than likely exceed the amount of computer time necessary to accomplish the same degree of refinement.

Certain limitations of the method are readily apparent. The exact form of the equations of motion must be known in order to construct the analog. The application of the method to more complex aircraft would require further investigation and refinement; for example, any nonlinear effects of the aircraft system would have to be duplicated by electronic circuitry in the analog. The accuracy obtainable for those derivatives to which the response is insensitive is undoubtedly of low order, but the possibility does exist of using different types of flight tests to establish these values. If these tests were compatible with the proposed data collection and reduction method, the additional effort could be minimized.

CONCLUSIONS AND RECOMMENDATIONS

The proposed method of extracting stability derivatives from transient flight data was proved to be feasible within the scope of this investigation. Matching of responses between the test aircraft and the equations of motion containing the derivatives is an excellent criterion for many applications of the derivatives. Due to the compatibility of the data collection system and the analog computer, the method is relatively fast and free from computational error. Only rough approximations to the values of the stability derivatives are needed to construct the analog. In general the accuracy with which each of the derivatives is obtained is associated with the importance of that stability derivative in influencing the motion of the aircraft during the test. The use of four different types of control deflections as forcing functions is considered a minimum requirement for accurate determination of all lateral derivatives. Subject to these restrictions, the exact form of each particular control deflection is arbitrary. Application of this method should include the preliminary procedures described under "Development of Method of Analysis" and "Preliminary Test of Feasibility of Method."

Application of this method to non-linear aircraft would require further investigation and refinement. Any non-linear effects in the aircraft system would have to be duplicated by electronic circuitry in the analog.

As a result of the investigation, the following recommendations are proposed:

1. Investigate the method at other flight conditions and with more complex aircraft.
2. Investigate the use of other control deflections to obtain responses which are more strongly influenced by the less sensitive derivatives. As an example, C_{l_r} might be more accurately obtained from an analysis of the response to a rudder step function.
3. Apply an initial condition such as a steady sideslip, prior to forcing the airplane with an aileron step function.
4. Augment the data (Table III) which indicates the effect(s) of the individual derivatives on the response of the system by conducting a similar variation of the derivatives when forcing the computer problem with an aileron function.
5. Improve the test aircraft aileron instrumentation by recording both left and right aileron angles and converting to average aileron angle by means of analog computer scaling circuits.

REFERENCES

1. Advisory Group for Aeronautical Research and Development Flight Test Manual, Volume II, Stability and Control, Edited by Perkins, Courtland D., Princeton University, 1954.

2. Triplett, William C., and Brown, Stuart C.: Lateral and Directional Dynamic Response Characteristics of a 35° Swept-Wing Airplane as Determined from Flight Measurements. NACA RMA52117, 1952.

3. Hall, Ian A. M., and Reynolds, Philip A.: An Investigation of a Simple Technique for Obtaining Lateral Stability Parameters by Dynamic Flight Tests. Princeton University Aeronautical Engineering Report No. 309, 1955.

4. Klein, H., and Sedney, R.: Some Basic Concepts for Analyzing Dynamic Flight Test Data. Douglas Aircraft Company Report No. SM-14511, 1952.

5. Perkins, Courtland D., and Hage, R. E.: Airplane Performance Stability and Control. John Wiley and Sons, New York, N. Y., 1949.

6. Advisory Group for Aeronautical Research and Development Flight Test Manual, Volume IV, Instrumentation Systems, Edited by Durbin, Enoch J., Princeton University, 1957.

7. Campbell, John P., and McKinney, M. O.: Summary of Methods for Calculating Dynamic Lateral Stability and Response and for Estimating Lateral Stability Derivatives. NACA Report 1098, 1952.

8. Dynamic Stability of Aircraft; Department of Aeronautics, U. S. Naval Postgraduate School, Monterey, Calif., 1953.

9. Smith, Robert P., and Vogt, L. F., Jr.: Determination of the Static Lateral and Directional Derivatives of an Airplane by Steady State Flight Testing. Princeton University Aeronautical Engineering Report No. 302, 1954.

10. Sweberg, Harold H., Guryansky, E.R., and Lange, Roy H.: Langley Full-Scale Tunnel Investigation of the Factors Affecting the Directional Stability and Trim Characteristics of a Fighter-Type Airplane. NACA ARR L5H09, 1945.

11. Pearson, Henry A., and Jones, R. T.: Theoretical Stability and Control Characteristics of Wings with Various Amounts of Taper and Twist. NACA Rep. 635, 1938.

12. Zimmerman, Charles H.: An Analysis of Lateral Stability in Power-Off Flight with Charts for Use in Design. NACA Rep. 589, 1937.

13. Stough, Carl J., and Kauffman, William M.: A Flight Investigation and Analysis of the Lateral-Oscillation Characteristics of an Airplane. NACA TN 2195, 1950.

14. Tamburello, Vito, and Weil, J.: Wind-Tunnel Investigation of the Effect of Power and Flaps on the Static-Lateral Characteristics of a Single-Engine Low-Wing Airplane Model. NACA TN 1327, 1947.

15. Williams, James L.: Measured and Estimated Lateral Static and Rotary Derivatives of a 1/12-Scale Model of a High-Speed Fighter Airplane with Unswept Wings. NACA RM L53K09, 1954.

16. Heinle, Donovan R., and McNeill, W. E.: Correlation of Predicted and Experimental Lateral Oscillation Characteristics for Several Airplanes. NACA RM A52J06, 1952.

17. Lappi, U. P.: A Fourier Integral Method for Obtaining the Sinusoidal Frequency Response from a Unit Step Transient. Cornell Aeronautical Laboratory FRM No. 30, 1947.

18. Seckel, E.: Suggested Procedure for Using the Corradi Analyzer to Obtain Airplane Frequency Responses from Transient Data. Cornell Aeronautical Laboratory FRM No. 104, 1950.

19. Lees, S.: Graphical Aids for the Graphical Representation of Functions of Imaginary Argument. Massachusetts Institute of Technology Instrumentation Laboratory Engineering Memorandum E-25. 1951.

20. Ross, I. G., and Whitcomb, D. W.: The Lateral Motion of an Airplane in Response to Sinusoidally Varying Rolling and Yawing Moment Forcing Functions. Cornell Aeronautical Laboratory Report TB-405-F-5. 1947.

21. Donegan, James J., Robinson, Samuel W., and Gates, Ordway B.: Determination of Lateral-Stability Derivatives and Transfer-Function Coefficients from Frequency-Response Data for Lateral Motions. NACA Rep. 1225. 1955.

22. Seckel, E.: Suggested Methods of Analyzing Airplane Longitudinal Frequency Response Data, Including a Method (Utilizing Observed Tail Loads) for Resolving the Lumped Transfer Constants, b_o and k_o, into their Aerodynamic Components. Cornell Aeronautical Laboratory FRM No. 75. 1949.

23. Shinbrot, M.: A Least Squares Curve-Fitting Method with Applications to the Calculation of Stability Coefficients from Transient Response Data. NACA TN 2341. 1951.

24. Larrabee, E. E.: Application of the Time-Vector Method to the Analysis of Flight Test Lateral Oscillation Data. Cornell Aeronautical Laboratory FRM No. 189. 1953.

25. Eggleston, John M., and Mathews, Charles W.: Application of Several Methods for Determining Transfer Functions and Frequency Response of Aircraft from Flight Data. NACA Rep. 1204. 1954.

TABLE I

METHODS FOR ANALYSIS OF DYNAMIC FLIGHT TEST DATA

OBJECTIVE	FLIGHT TEST METHODS	RELATIVE FLIGHT TEST TIME	FORM OF RECORDED DATA	DATA CONVERTED TO	METHOD OF DATA CONVERSION	DATA FURTHER CONVERTED TO	METHOD OF CONVERSION	RELATIVE DATA ANALYSIS TIME	USEFULNESS OF RESULTS IN FINAL FORM	REFERENCE (•) (•) INDICATES REFERENCE NUMBER TO THIS REPORT
TRANSIENT RESPONSE	CONTROL PULSE OR STEP	VERY SHORT	TIME HISTORY OF TRANSIENT RESPONSE	-------	-------	-------	-------	-------	COMPARISON OF PREDICTED AND ACTUAL DYNAMIC RESPONSE, & DETERMINATION OF ACTUAL DEGREE OF DYNAMIC STABILITY	AGARD VOL. II, (1)
FREQUENCY RESPONSE	(A) FORCED OSCILLATION	(A) LONG	TIME HISTORY OF (A) STEADY STATE OSCILLATION	(A) FREQUENCY RESPONSE	(A) REPLOT OF AMPLITUDE RATIO AND PHASE ANGLE	-------	-------	(A) SHORT	CORRECTIONS FOR DYNAMIC RESPONSE OF RECORDING INSTRUMENTATION EASILY APPLIED	(A) CAL TB 405-F5, (20)
	(B) CONTROL PULSE OR STEP	(B) VERY SHORT	(B) TRANSIENT RESPONSE	(B) FREQUENCY RESPONSE	(B) HARMONIC ANALYSIS	-------	-------	(B) LONG		(B) CAL FRM NO. 30, (17) CAL FRM NO.104, (18) NACA TR 1204, (25)
TRANSFER FUNCTION COEFFICIENTS	(A) FORCED OSCILLATION	(A) LONG	TIME HISTORY OF (A) STEADY STATE OSCILLATION	(A) FREQUENCY RESPONSE	(A) REPLOT OF AMPLITUDE RATIO AND PHASE ANGLE	TRANSFER FUNCTION COEFFICIENTS	(A) AND (B_1): ANALYTICAL OR GRAPHICAL CURVE FITTING TO TRANSFER FUNCTION PLOTS, OR USE OF DYNAMIC RESPONSE TEMPLATES	LONG	DESIGN OF AUTOPILOT AND ARTIFICIAL STABILITY EQUIPMENT, AND FLIGHT SIMULATORS	(A) MIT EM E-25, (19)
	(B) CONTROL PULSE OR STEP	(B) VERY SHORT	(B) TRANSIENT RESPONSE	(B) FREQUENCY RESPONSE	(B_1) HARMONIC ANALYSIS	TRANSFER FUNCTION COEFFICIENTS				
					(B_2) HARMONIC ANALYSIS, USING DIGITAL COMPUTER	TRANSFER FUNCTION COEFFICIENTS	(B_2) DYNAMIC RESPONSE TEMPLATES, AND MATCHING OF TIME HISTORIES TO FLIGHT DATA ON ANALOG COMPUTER			(C) NACA RM A52117; (2)
STABILITY DERIVATIVES	(A) FORCED OSCILLATION	(A) LONG	(A) TIME HISTORY OF STEADY STATE OSCILLATION	(A) FREQUENCY RESPONSE	(A) REPLOT OF AMPLITUDE RATIO AND PHASE ANGLE	(A) CIRCLE DIAGRAM	(A) FURTHER REPLOT OF AMPLITUDE RATIO AND PHASE ANGLES	(A) LONG	COMPARISON OF PREDICTED, WIND TUNNEL, AND FULL SCALE FLIGHT TEST VALUES FOR DERIVATIVES. ACTUAL DERIVATIVES ARE ALSO OFTEN OF MORE VALUE IN ANALYSIS AND DESIGN OF AUTOPILOT AND CONTROL EQUIPMENT THAN ARE TRANSFER FUNCTIONS	(A) CAL TB 405-F5, (20)
	(B) FORCED OSCILLATION	(B) LONG	(A) TIME HISTORY OF STEADY STATE OSCILLATION	(B) FREQUENCY RESPONSE	(B) REPLOT OF AMPLITUDE RATIO AND PHASE ANGLE	(B) STABILITY DERIVATIVES	(B) VECTOR TECHNIQUE, AND LEAST SQUARES (LATERAL MODE ONLY)	(B) VERY LONG		(B) NACA TR 1225, (21)
	(C) FORCED OSCILLATION OR PULSE		(C) (A) OR (D)	(C) FREQUENCY RESPONSE	(C) SAME AS (A), OR HARMONIC ANALYSIS	(C) STABILITY DERIVATIVES	(C) TAIL-OFF & TAIL-ON LOAD MEASUREMENTS (LONGITUDINAL MODE)	(C) SHORT		(C) CAL FRM NO. 75, (22)
	(D) CONTROL PULSE OR STEP	(D) VERY SHORT	(D) TIME HISTORY OF TRANSIENT RESPONSE	(D) -------	-------	(D) STABILITY DERIVATIVES	(D) APPLICATION OF LEAST SQUARES	(D) LONG		(D) NACA TN 2341; (23)
	(E) CONTROL PULSE	(E) VERY SHORT	(E) TIME HISTORY OF TRANSIENT RESPONSE	(E) AMPLITUDE RATIOS AND PHASE ANGLES	(E) SEMI-LOG PLOTS	(E) STABILITY DERIVATIVES	(E) GRAPHICAL PLOT OF TIME-VECTOR POLYGONS	(E) LONG		(E) CAL FRM NO.189 (24)

TABLE II

PHYSICAL CHARACTERISTICS OF NAVION

A.	**WING**	
1.	Total Wing Area, S_W (includes flaps, ailerons and 19.87 Ft.^{2} covered by the fuselage)	184.337 Ft.^{2}
2.	Span b_W	33.378 Ft.
3.	MAC	68.352 in.
4.	Angle of Incidence	
	Root, i_r	+2°
	Tip, i_t	-1°
5.	Twist	
	Aerodynamic	2° 31'
	Geometric	3°
6.	Airfoil Section	
	Root	NACA 4415R
	Tip	NACA 6410R
7.	Aspect Ratio, AR_W	6.044
8.	Taper Ratio, λ_W	0.5265
9.	Dihedral	7.5°
10.	Root Chord	7.2 Ft.
11.	Tip Chord	3.92 Ft.
A-1.	**AILERON** (one Aileron only) (Beaded skin, Frise Nose Balance, No Trailing Edge Extension)	120°-120° Wheel Throw Fixed bend tab on right aileron.
1.	Area, S_a	2.161 Ft.^{2}
2.	Span, b_a	61.987 in.
3.	Aileron Deflection, δ_a	30° UP, 20° DN.
4.	Boost	None
5.	Trim Tab	Fixed bend tab on right aileron.

B. HORIZONTAL TAIL

1. Total Area (Includes 2.368 Ft.^{2} covered by fuselage)	43.051 Ft.^{2}
2. Span, b_H	13.172 Ft.
3. Airfoil Section	NACA 0012
4. Taper Ratio, λ_t	.67
5. MAC, $\bar{c}_t$	3.34 Ft.
6. Aspect Ratio, AR_t	4.02

B-1. HORIZONTAL STABILIZER

1. Area, S_s	28.953 Ft.^{2}
2. δ_H (with reference to FRP)	-4°

B-2. ELEVATORS

(No Trailing Edge Extensions)

Smooth Skin
Flat sided
No trim bungee
Balance spring

1. Total Area, S_e	14.098 Ft.^{2}
2. Span, b_e	73.582 in.
3. Deflection, δ_e	30° UP, 20° DN.
4. Trim Tabs (32" Span, 4-1/2" Chord)	30° UP, 30° DN.
5. Root Chord	1.5 Ft.
6. Tip Chord	1.0 Ft.

C. VERTICAL TAIL

1. Total Area, S_v (Includes 2.577 Ft.^{2} blanketed by fuselage and excluding 1.483 Ft.^{2} of dorsal fin)	12.925 Ft.^{2}
2. Airfoil Section	
Root	NACA 0013.2 Mod.
Tip	NACA 0012-64 "

C-1. VERTICAL STABILIZER

1. Area, S_{v_s} (Includes 0.1427 Ft.^{2} blanketed by fuselage)	6.873 Ft.^{2}
2. α (With reference to fuselage Ø)	2° Nose left

C-2. RUDDER

	Smooth Skin Rigged 3° Rt. to Fin Ø, Fixed Bend Tab.
1. Area, S_r	6.052 Ft.^{2}
2. Rudder Deflection, δ_r	17° L - 23° R
3. Rudder Pedal Throw	5.75 in.
4. Trim Tab	Fixed Bend Tab

D. PROPELLER

	Hartzell
1. Activity Factor, A.F.	100
2. Diameter, d	86"
3. Pitch θ @ .75 R	21° 30'

E. NOSE GEAR

1. Travel	± 30°
2. Strut Angle (To Vertical)	10°

F. MISCELLANEOUS

1. Length, overall	27.25 Ft.
2. Tail length, l_{VT}	16.88 Ft.

G. POWER

1. Engine	Continental E-185 Engine 185 HP @ 2300 RPM, 29" Hg M.P. @ Sea Level

TABLE III-a

EFFECT OF VARIATION OF STABILITY DERIVATIVES ON AIRCRAFT RESPONSE (1)

PARAMETER INCREASE	PEAK MAGNITUDE OF:			PERIOD	$T_{1/2}$
	β	$\dot{\psi}$	$\dot{\phi}$		
C_{n_r}	decrease	decrease	decrease	-	strong decrease
C_{l_r}	-	-	-	-	slight decrease
C_{n_p}	-	-	-	slight decrease	-
C_{l_p}	-	-	strong decrease	slight increase	slight decrease
C_{l_β}	-	-	strong increase	slight decrease	moderate increase
C_{y_β}	slight decrease	slight decrease	slight decrease	-	small decrease
C_{n_β}	decrease	decrease	decrease	strong decrease	-
$C_{n_{\delta r}}$	increase	increase	increase	-	-
$C_{l_{\delta r}}$	-	-	-	-	-
$C_{y_{\delta r}}$	-	-	-	-	-

---

(1) Only rudder forcing function used.

TABLE III-b

STABILITY DERIVATIVES WHICH INFLUENCE SPECIFIC ASPECTS OF AIRCRAFT RESPONSE

PEAK MAGNITUDE OF:			PERIOD	DAMPING
β	$\dot{\psi}$	$\dot{\phi}$		
$C_{n_{\delta_r}}$	$C_{n_{\delta_r}}$	$C_{n_{\delta_r}}$	(C_{n_β})	C_{n_r}
(C_{n_β})	(C_{n_β})	C_{l_β}	(C_{l_β})	(C_{l_β})
(C_{n_r})		(C_{l_p})	(C_{n_p})	C_{l_p}
		(C_{n_β})	C_{l_p}	C_{y_β}

Derivatives listed in descending order of effect.

( ) -- Indicates a decrease in the variable affected.

TABLE IV

PRIMARY EFFECTS OF INDIVIDUAL STABILITY DERIVATIVES ON AIRCRAFT RESPONSE

CONTROLLING DERIVATIVE	RESPONSE CHARACTERISTICS
C_{n_β}	Period of the Dutch roll mode.
C_{n_r}	Damping of the Dutch roll mode.
$C_{n_{\delta_r}}$	Magnitude of $\dot{\psi}$ and β response to a rudder deflection.
C_{l_β}	Phase and amplitude of the $\dot{\phi}$ response to a rudder deflection.
$C_{l_{\delta_a}}$	Amplitude of initial $\dot{\phi}$ response to an aileron step input.
C_{l_p}	Having established a value for $C_{l_{\delta_a}}$, C_{l_p} can be determined by the roll response to an aileron doublet, particularly during the last half of the control input.
$C_{l_{\delta_r}}$	Adverse roll characteristics, which are apparent in the $\dot{\phi}$ response immediately after a rudder deflection.
C_{n_p} & $C_{n_{\delta_a}}$	An upper and lower limit for C_{n_p} can be established by an amplitude match of the $\dot{\psi}$ responses to a rudder deflection. C_{n_p} can then be adjusted within these limits along with the adjustments in $C_{n_{\delta_a}}$ to provide the best match of $\dot{\psi}$ response to an aileron doublet.

(continued)

TABLE IV (continued)

C_{l_r}	Response insensitive to this derivative, but a qualitive match of the slope of the mean response to an aileron step function is the best means available for determining C_{l_r} .
C_{y_β} & $C_{y_{\delta_r}}$	Response too insensitive to these derivatives to permit the determination of a special effect in either case.

TABLE V

THEORETICAL AND FINAL EXPERIMENTAL LATERAL STABILITY DERIVATIVES

Derivative	Theoretical Value	Final Experimental Value
C_{y_β}	-.592	-.592
C_{n_β}	.0613	.101
C_{l_β}	-.0814	-.0595
C_{n_p}	-.0510	-.0705
C_{l_p}	-.46	-.43
C_{n_r}	-.0937	-.0951
C_{l_r}	.102	.131
$C_{l_{\delta_r}}$	.0152*	.0069
$C_{n_{\delta_r}}$	-.0561	-.0774
$C_{y_{\delta_r}}$	.111	.144
$C_{l_{\delta_a}}$	.133	.137
$C_{n_{\delta_a}}$	-.0087	-.0031

* From Ref. 9

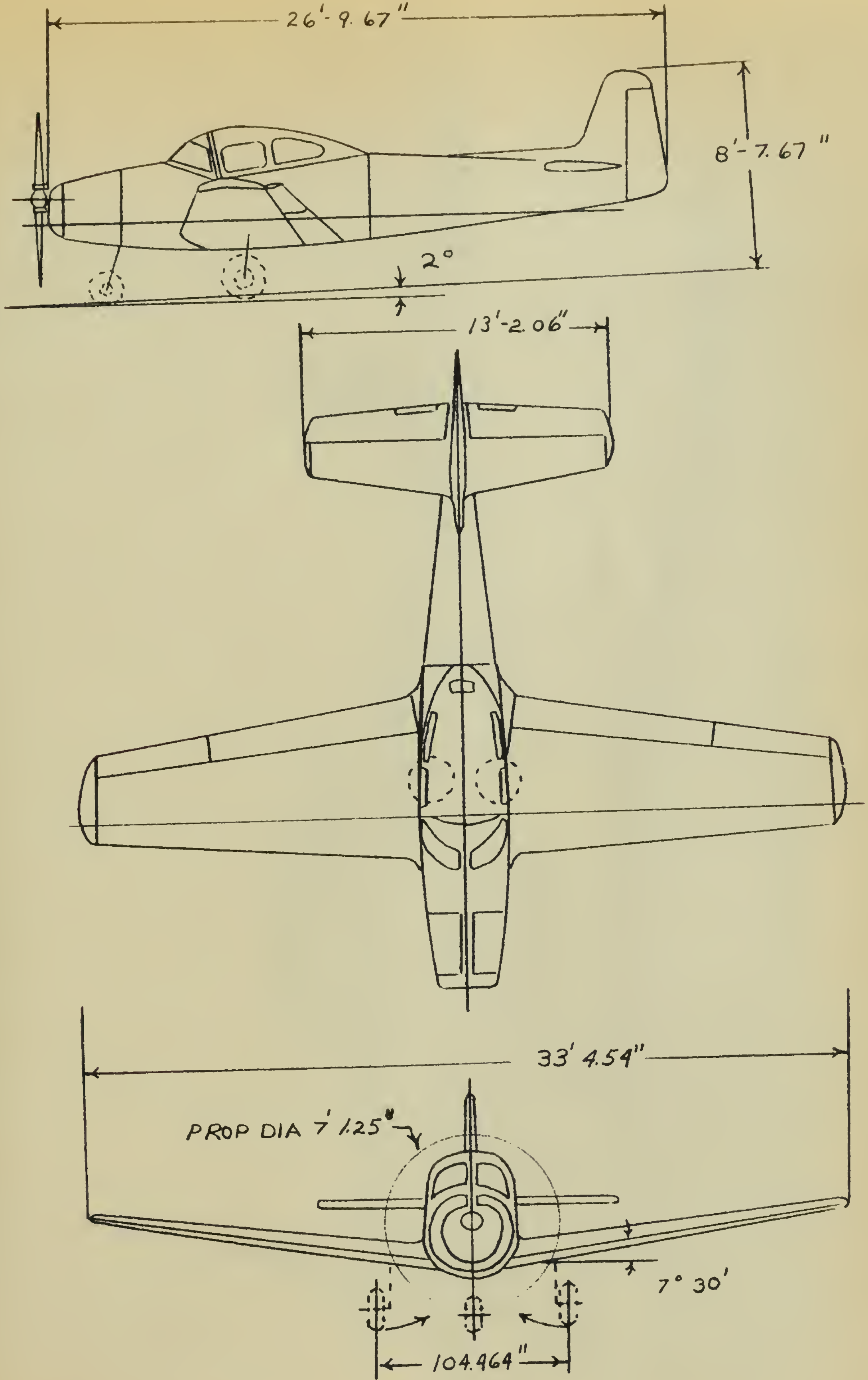

FIG 1

GENERAL THREE-VIEW DRAWING

FIGURE 2 - TEST AIRCRAFT

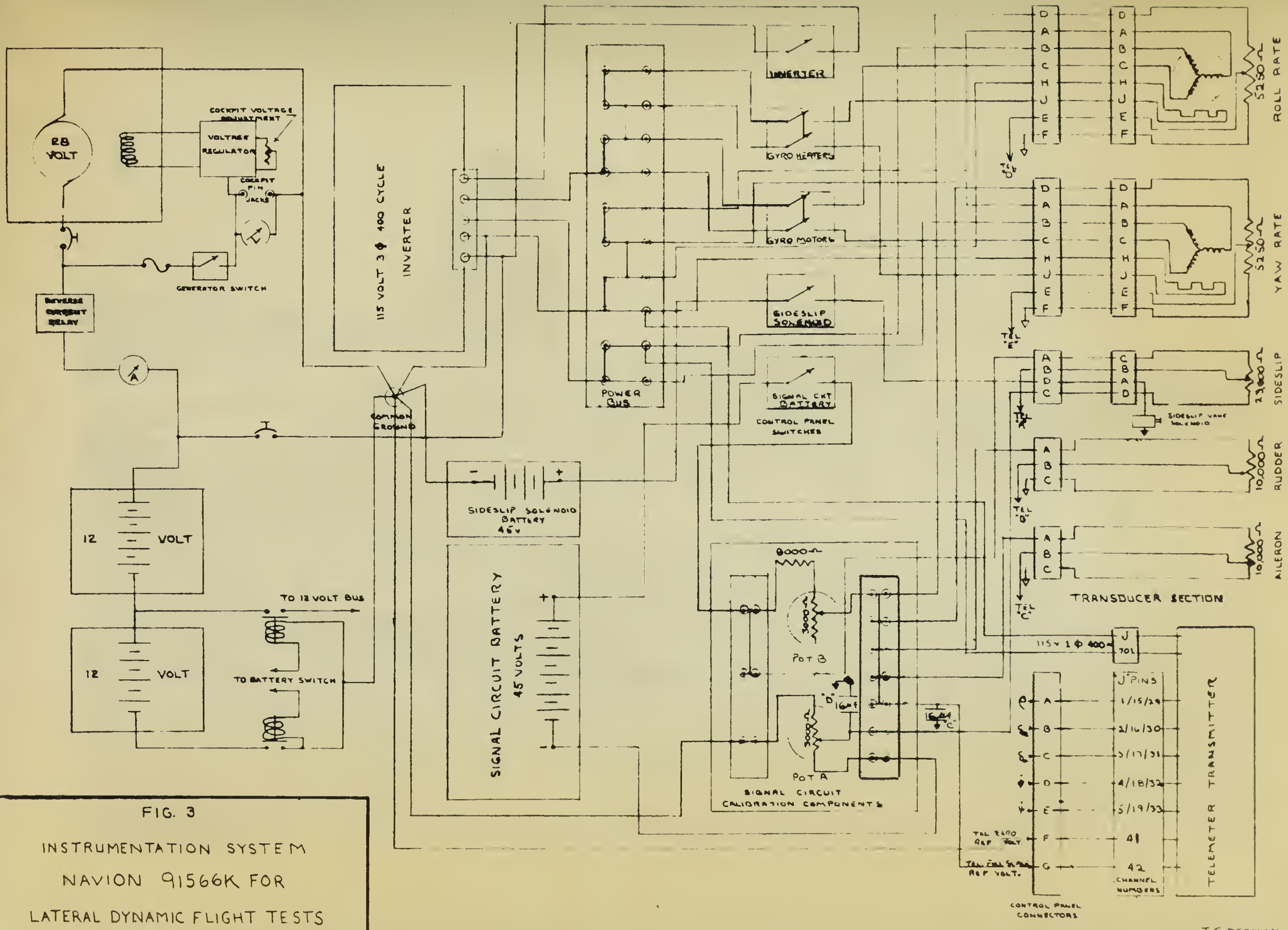

FIG. 3

INSTRUMENTATION SYSTEM
NAVION 91566K FOR
LATERAL DYNAMIC FLIGHT TESTS

T F DEDMAN

FIGURE 4 - SIDE-SLIP VANE AND RELEASE MECHANISM

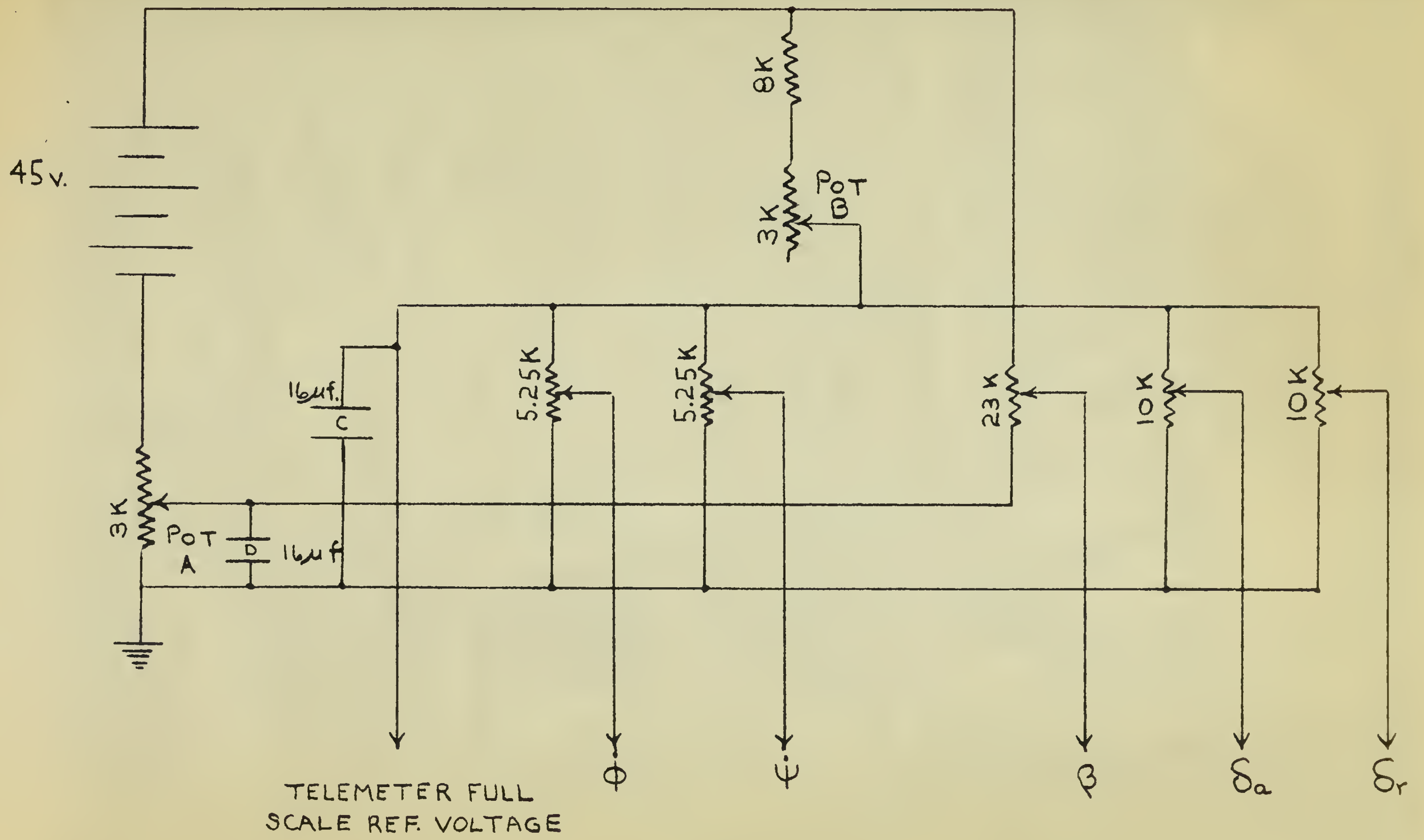

FIG 5

SCHEMATIC OF AIRCRAFT INSTRUMENTATION CIRCUIT

FIGURE 6A - TEST AIRCRAFT CABIN WITH INSTRUMENTATION INSTALLATION

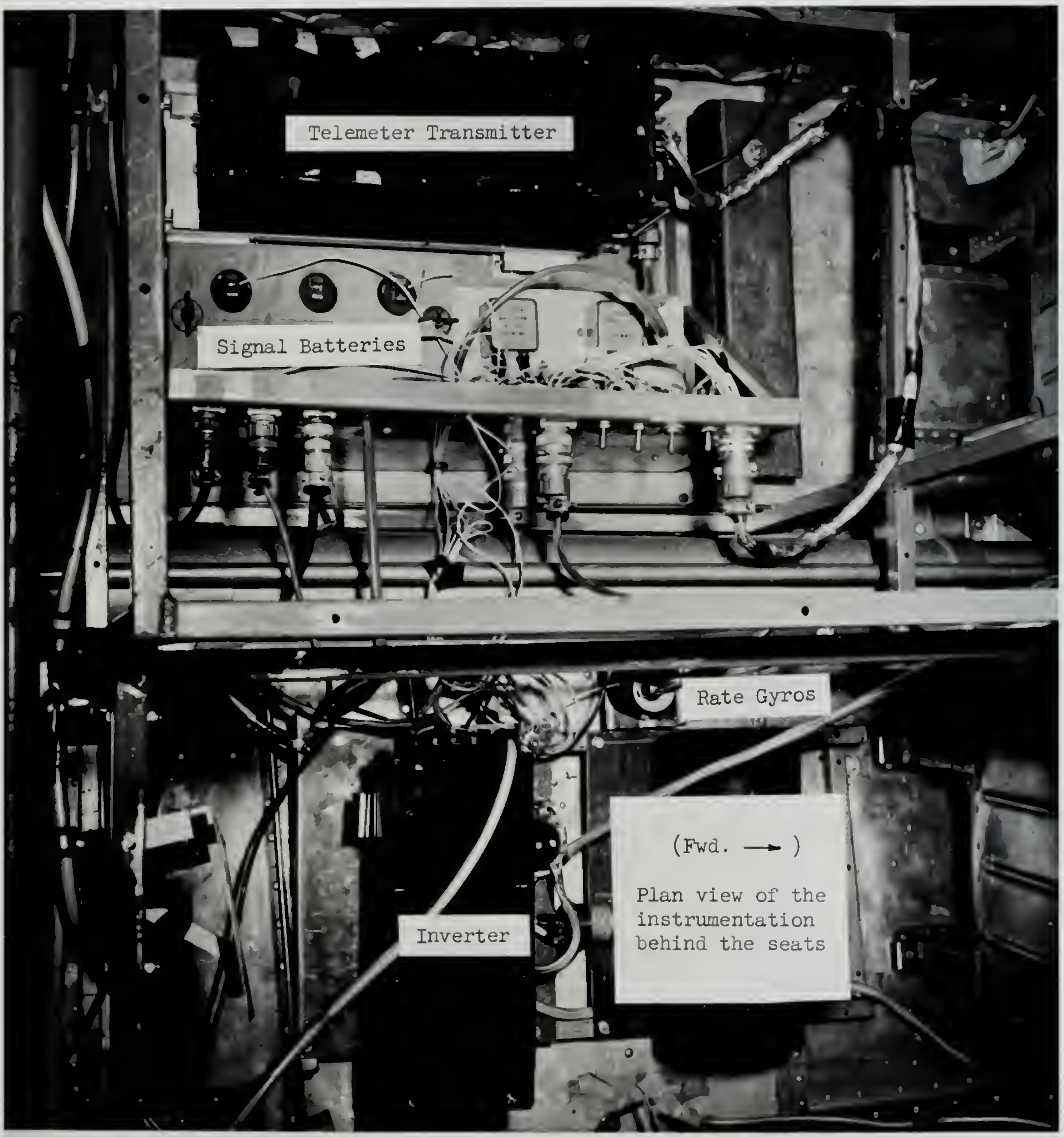

FIGURE 6B - TEST AIRCRAFT INSTRUMENTATION

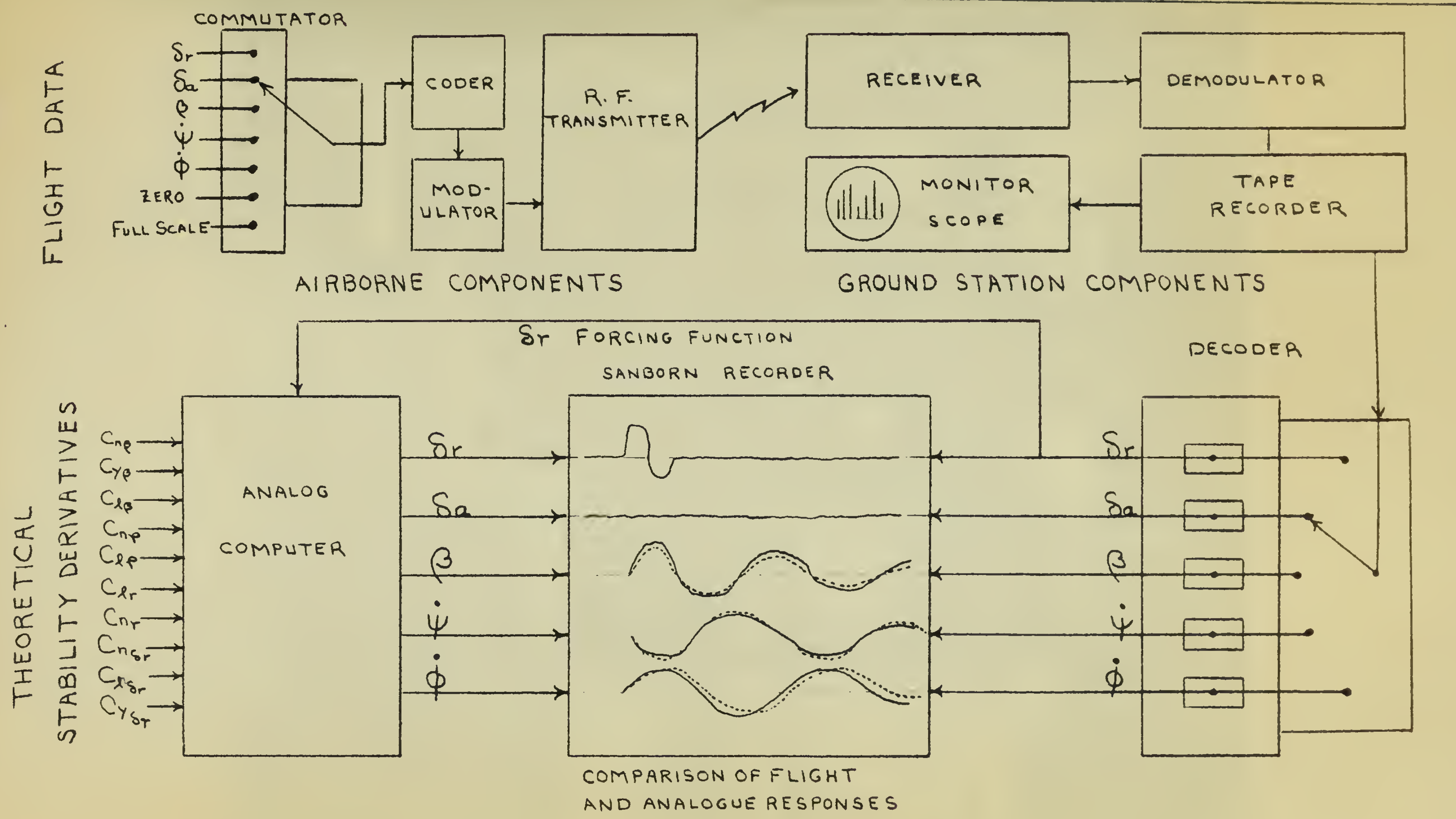

FIG 7

SCHEMATIC OF DATA COLLECTION AND ANALYSIS SYSTEMS

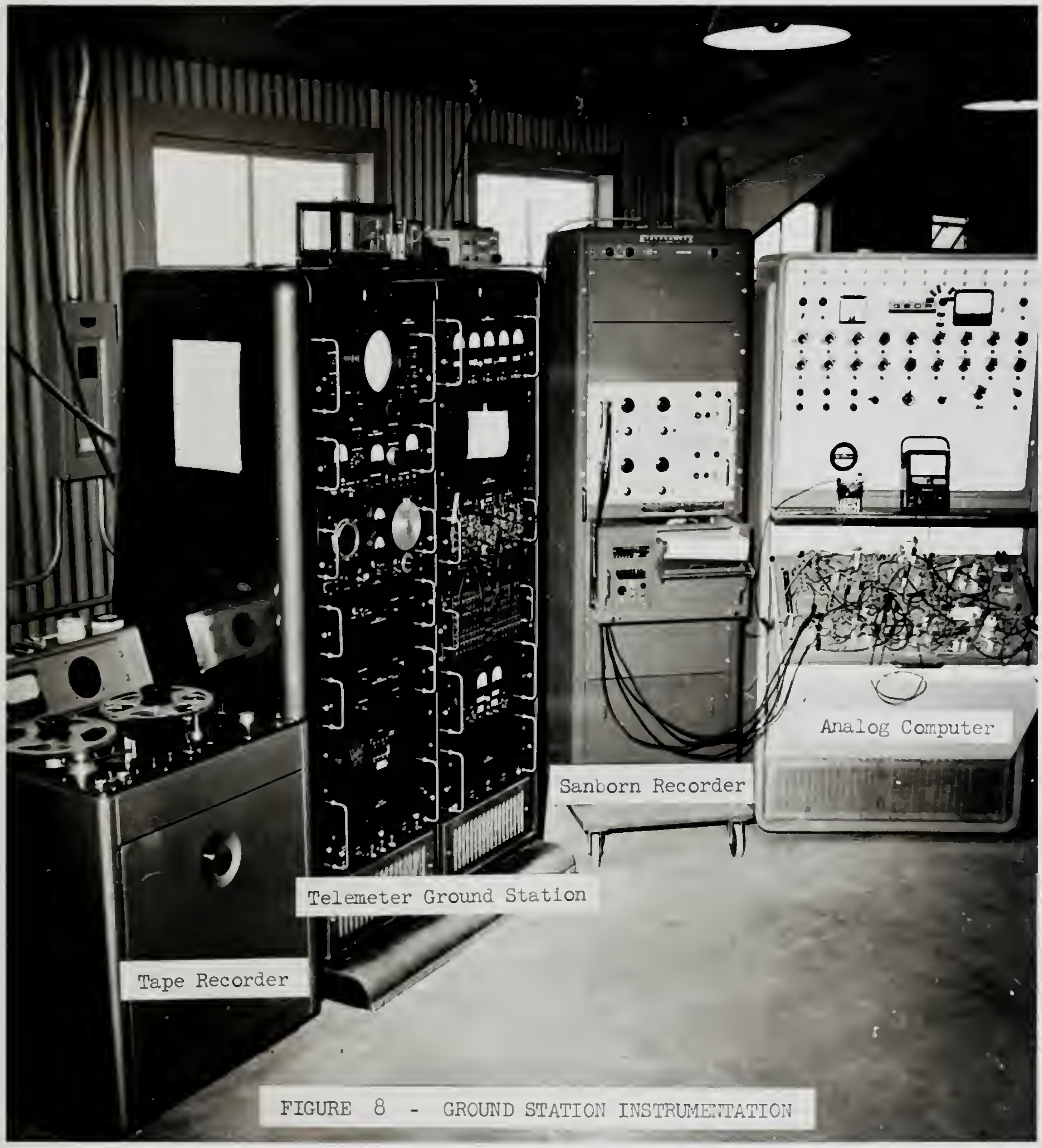

FIGURE 8 - GROUND STATION INSTRUMENTATION

FIG. 9

RATE GYRO CALIBRATION

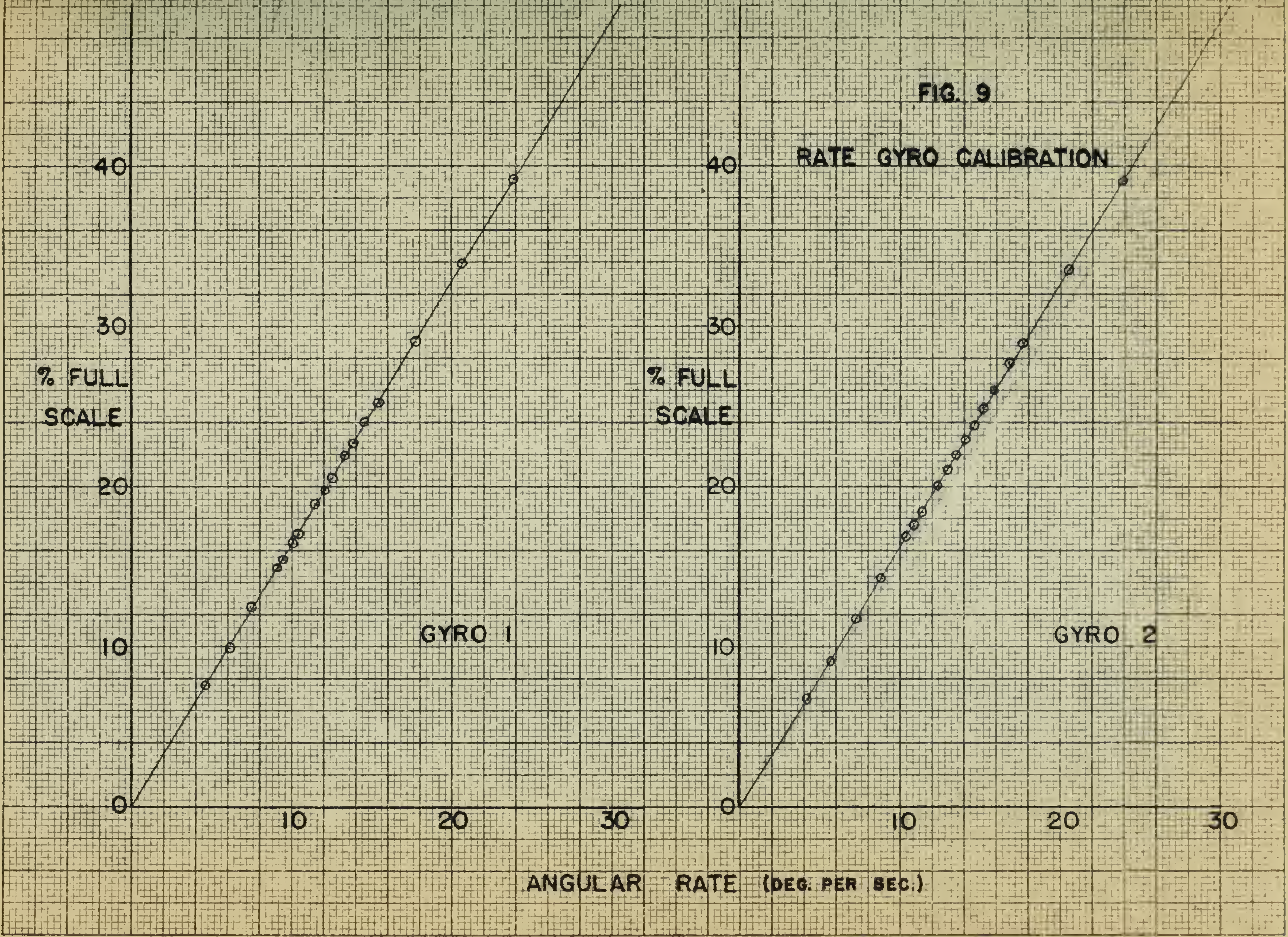

FIG. 10

SIDESLIP VANE CALIBRATION

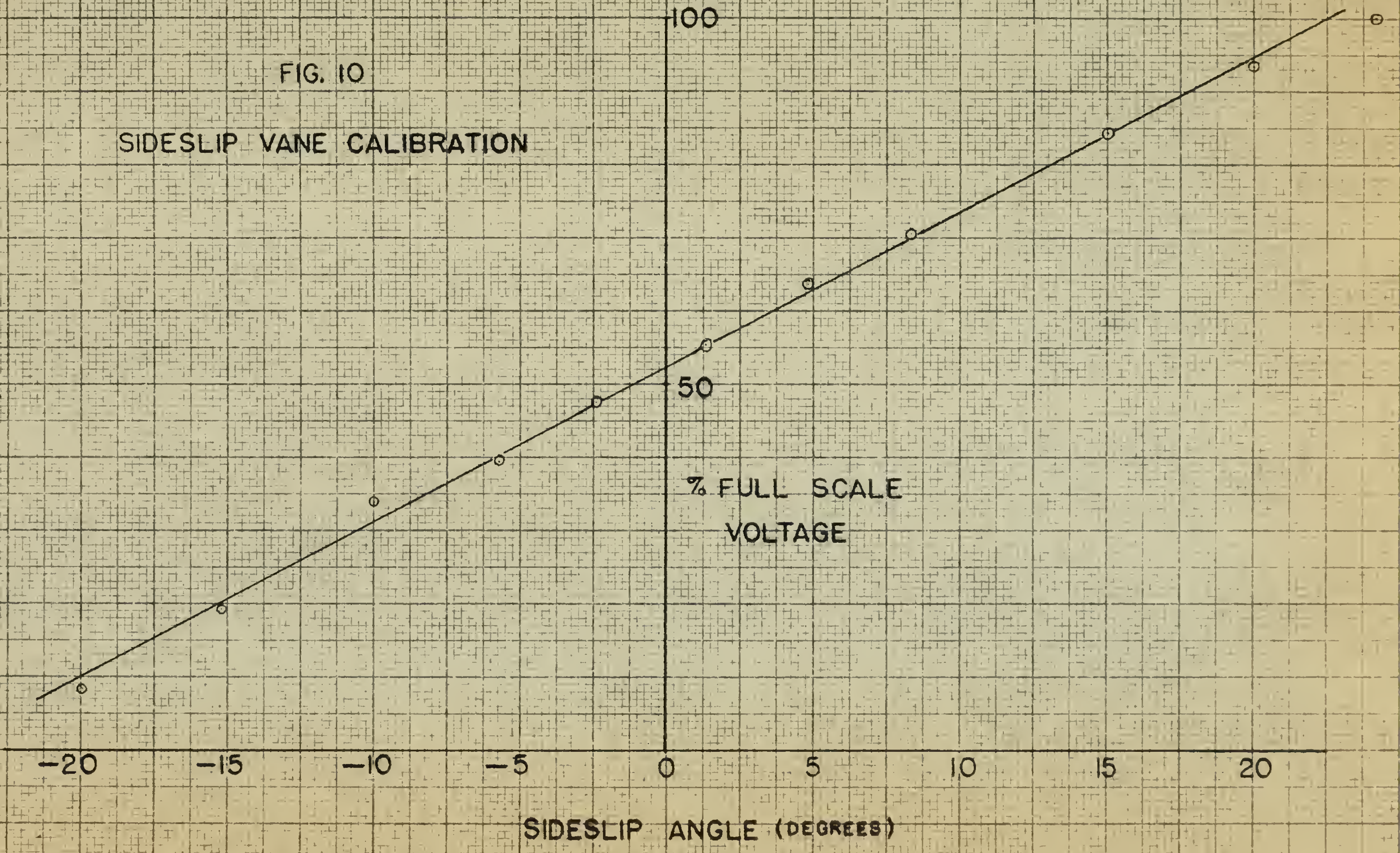

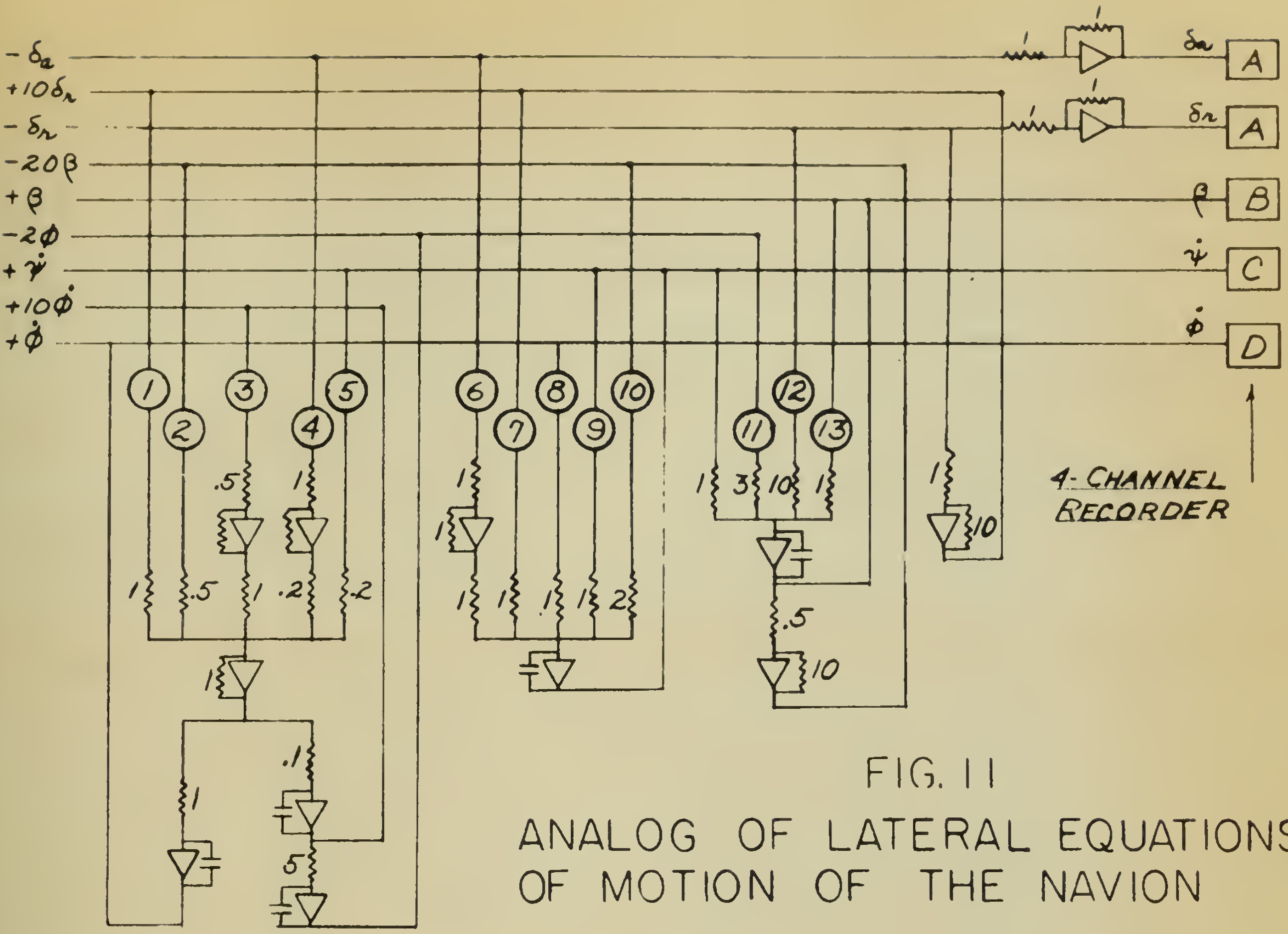

FIG. 11

ANALOG OF LATERAL EQUATIONS OF MOTION OF THE NAVION

Pot. Number	1	2	3	4	5	6	7	8	9	10	11	12	13
Represen-tation	$\frac{\mu C_{l\delta_r}}{\tau^2 J_x}$	$\frac{\mu C_{l\beta}}{\tau^2 J_x}$	$\frac{C_{lp}}{2\tau J_x}$	$\frac{\mu C_{l\delta_a}}{\tau^2 J_x}$	$\frac{C_{lr}}{2\tau J_x}$	$\frac{\mu C_{n\delta_a}}{\tau^2 J_z}$	$\frac{\mu C_{n\delta_r}}{\tau^2 J_z}$	$\frac{C_{np}}{2\tau J_z}$	$\frac{C_{nr}}{2\tau J_z}$	$\frac{\mu C_{n\beta}}{\tau^2 J_z}$	$\frac{C_L}{2\tau}$	$\frac{C_{y\delta_r}}{2\tau}$	$\frac{C_{y\beta}}{2\tau}$
Pot. Setting	21.8 $\times C_{l\delta_r}$	5.47 $\times C_{l\beta}$	0.95 $\times C_{lp}$	4.36 $\times C_{l\delta_a}$	3.80 $\times C_{lr}$	59.5 $\times C_{n\delta_a}$	6.51 $\times C_{n\delta_r}$	5.67 $\times C_{np}$	5.65 $\times C_{nr}$	6.51 $\times C_{n\beta}$	.257	4.21 $\times C_{y\delta_r}$	.421 $\times C_{y\beta}$

FIG. 12

POTENTIOMETER SETTINGS FOR ANALOG OF NAVION

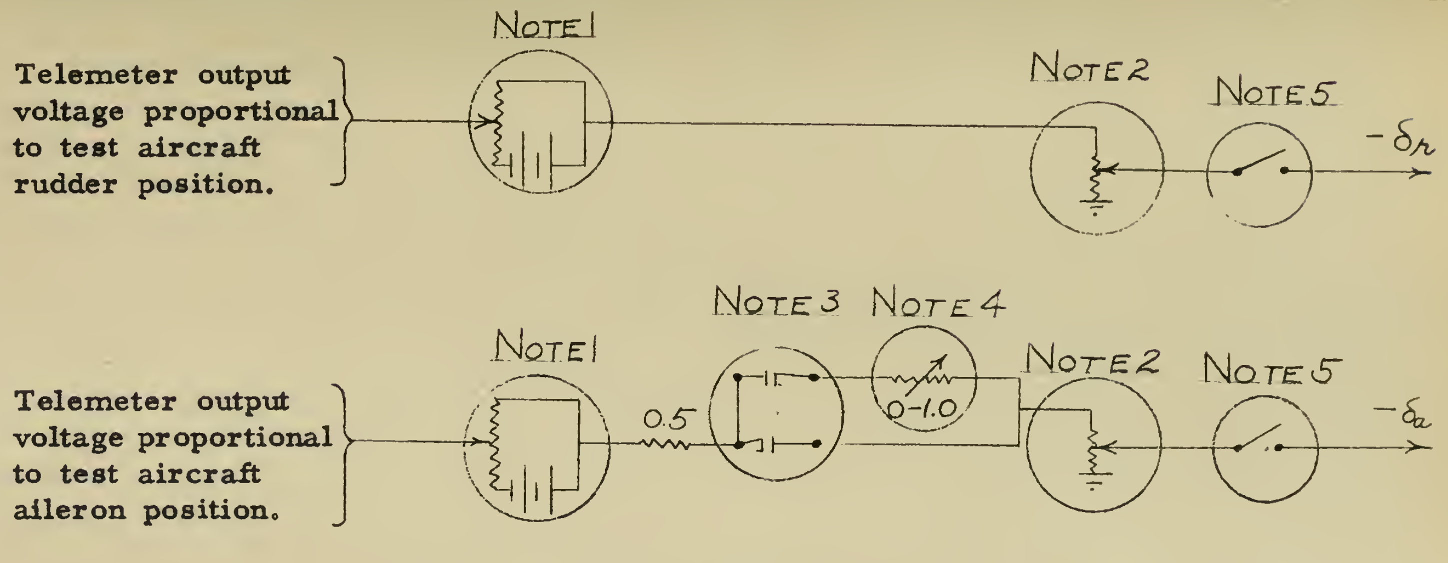

Note 1. Steady-state signal biased to zero voltage. Fine adjustment accomplished by assuring that steady-state signal had no effect on computer analog.

Note 2. Magnitude of signal adjusted to the scaling of the computer.

Note 3. Diodes effectively divided aileron signal into a left roll circuit and a right roll circuit.

Note 4. Variable resistor placed in right roll circuit to attenuate signal. This was done to correct a signal error caused by aileron cable stretch. See Appendix B for a complete explanation.

Note 5. Switch used to place forcing signal into the computer analog.

FIG. 13

COMPUTER FORCING FUNCTION CIRCUITS

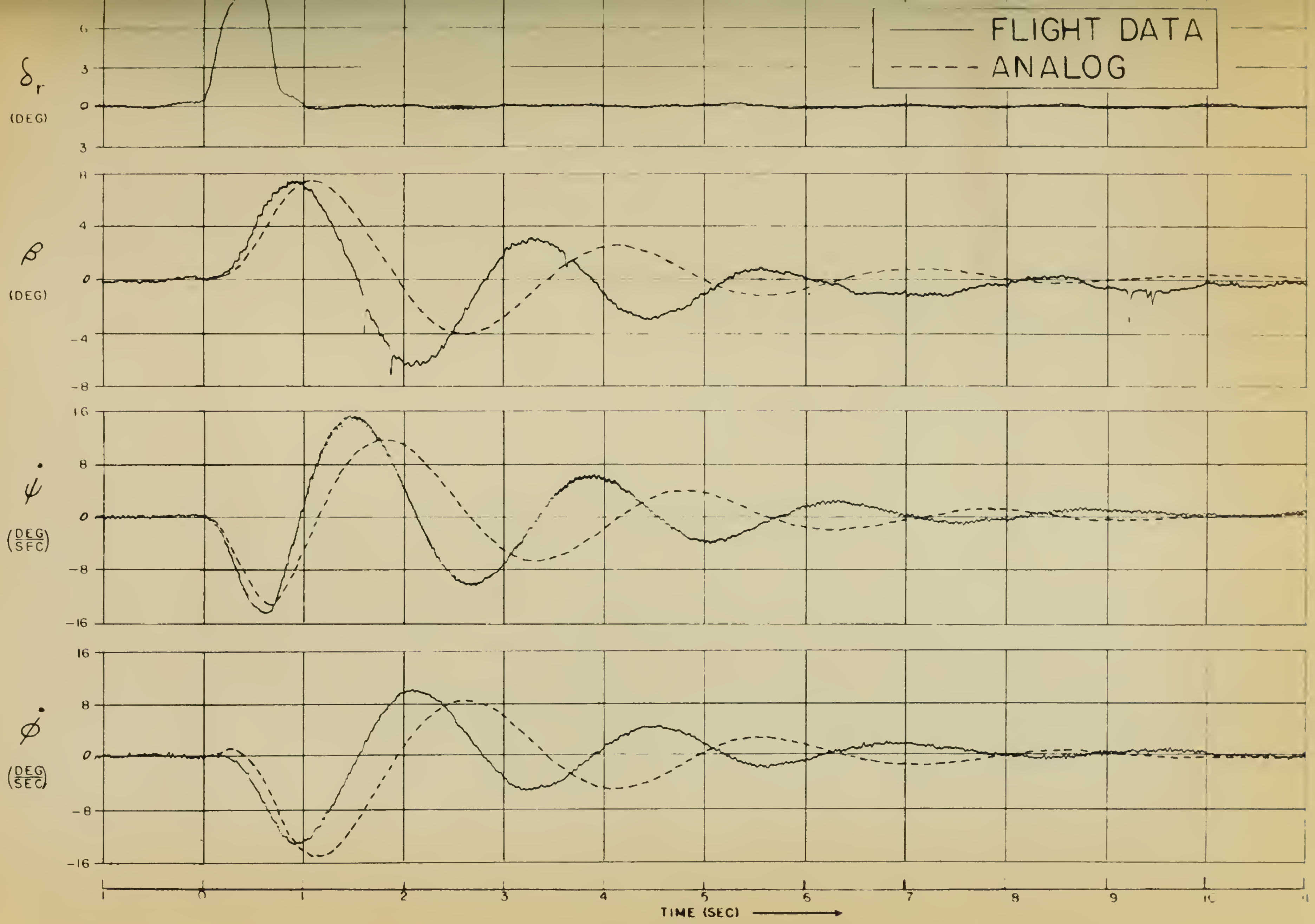

FIG. 14

INITIAL RESPONSE TO RUDDER PULSE
(THEORETICAL DERIVATIVES – TABLE V)

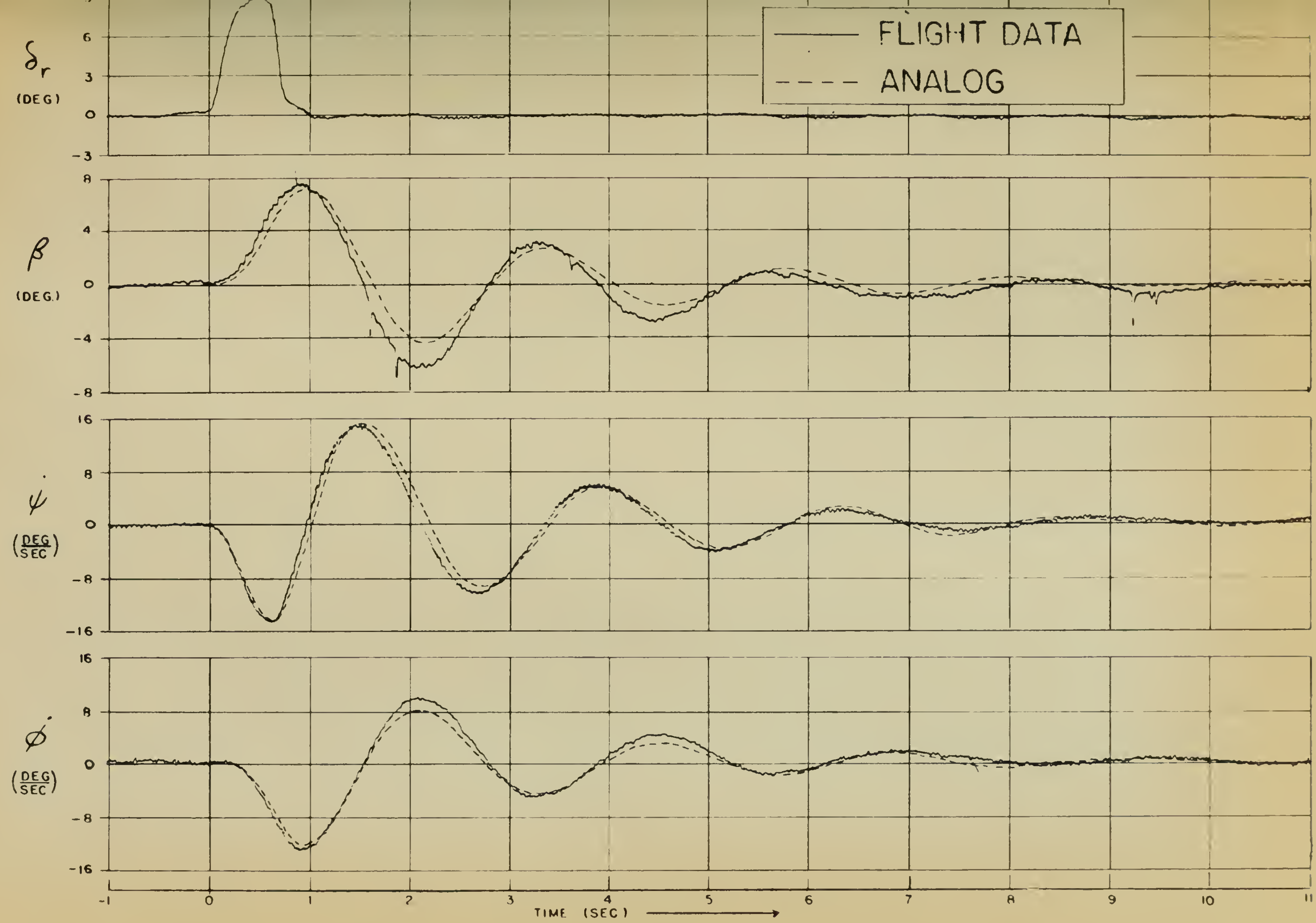

FIG. 15

MATCHED RESPONSE TO RUDDER PULSE

(FINAL STABILITY DERIVATIVES – TABLE V)

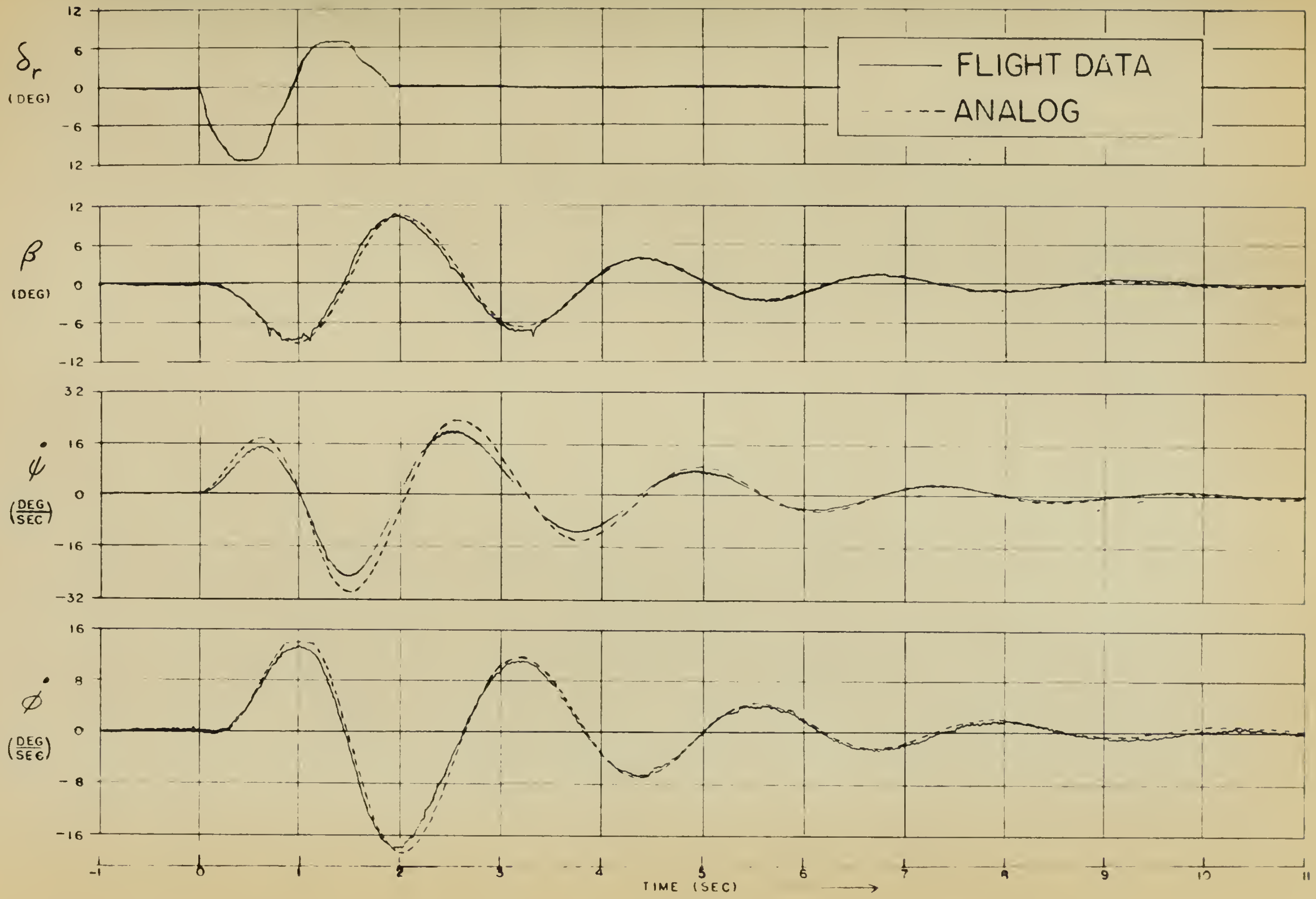

FIG. 16

MATCHED RESPONSE TO RUDDER DOUBLET
(FINAL STABILITY DERIVATIVES – TABLE V)

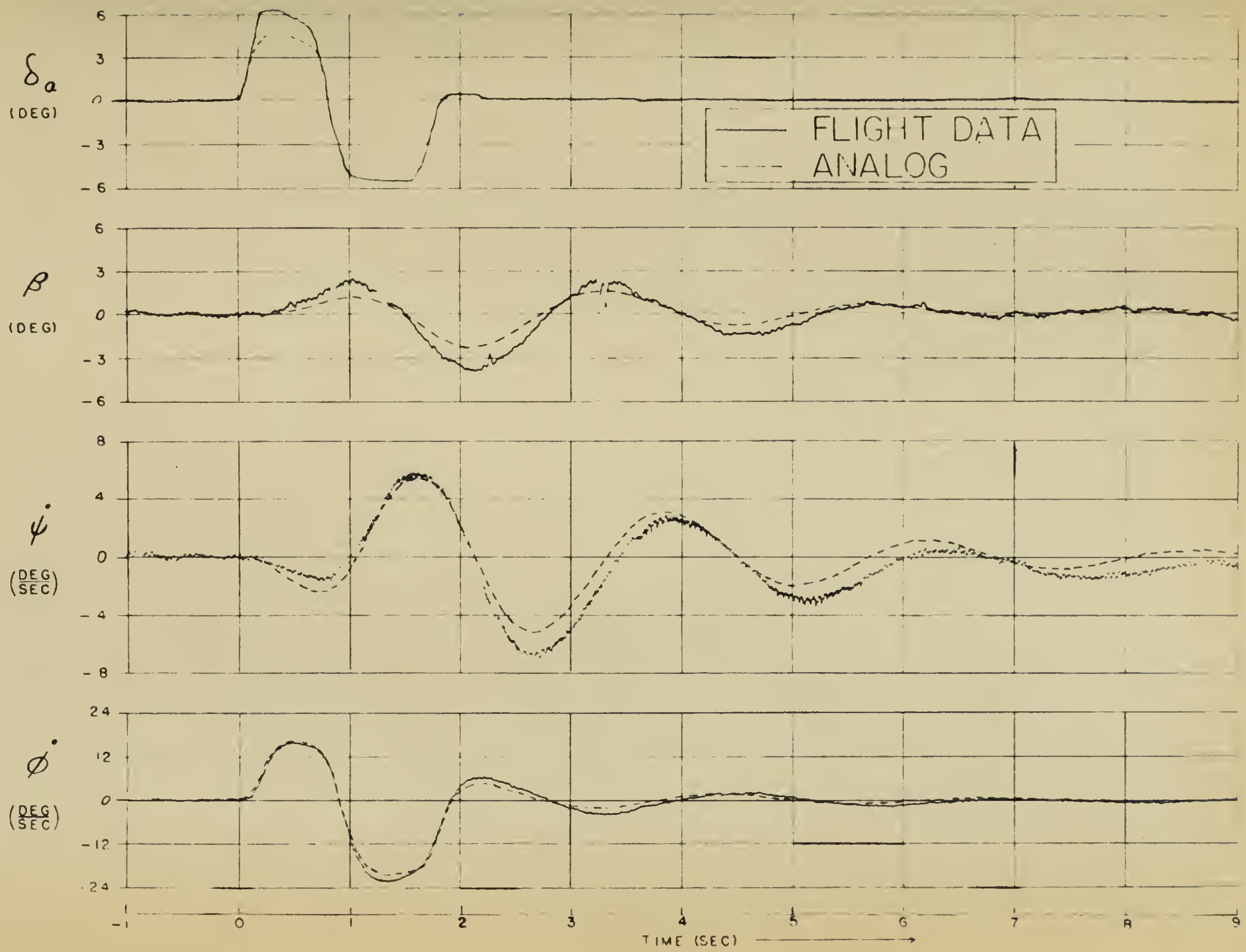

FIG 17

MATCHED RESPONSE TO AILERON DOUBLET
(FINAL STABILITY DERIVATIVES - TABLE V)

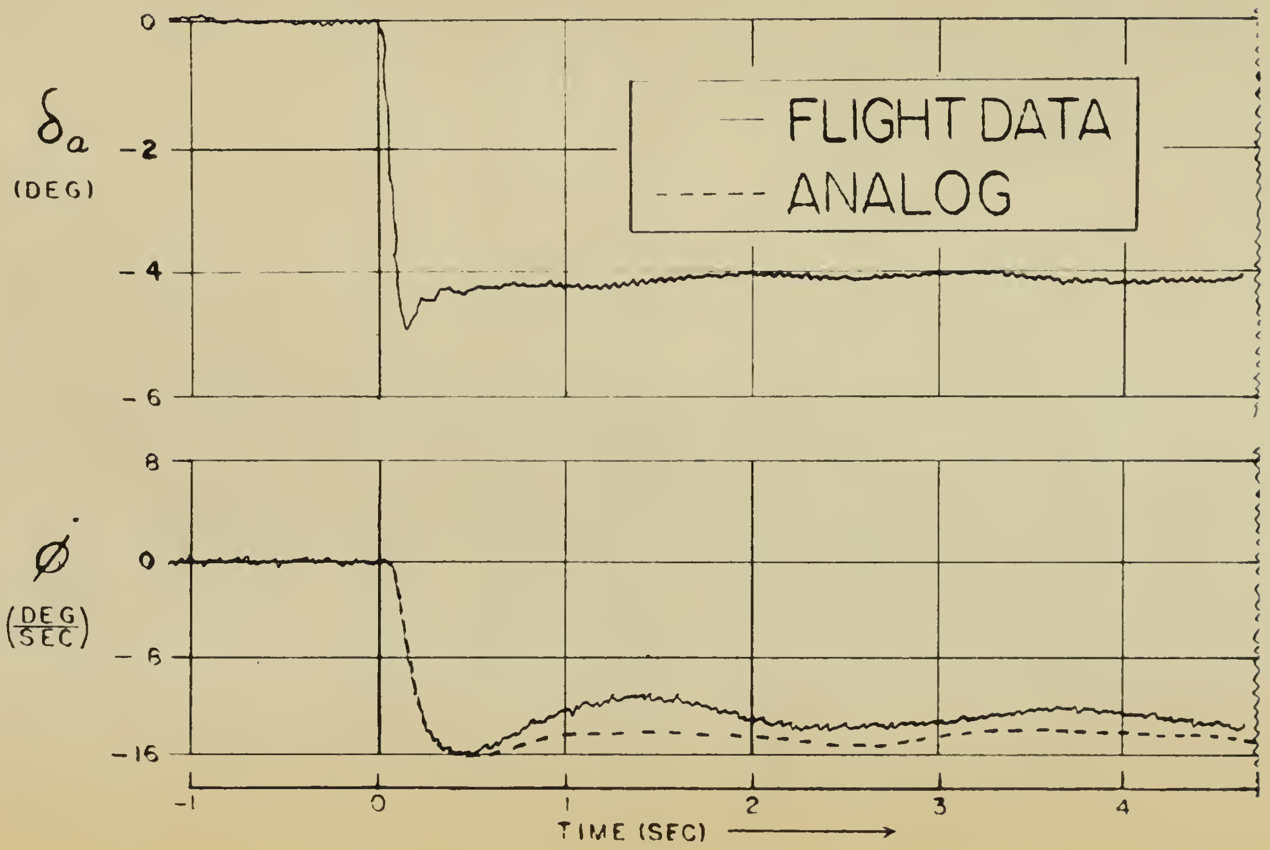

FIG. 18

MATCHED RESPONSE TO AILERON STEP FUNC.

(FINAL STABILITY DERIVATIVES – TABLE V)

APPENDIX A

THEORETICAL AND EXPERIMENTAL DETERMINATION OF THE DYNAMIC RESPONSE CHARACTERISTICS OF THE SIDESLIP VANE

General

The instrument system chosen for measurement of the sideslip angle consisted of a light vane mounted on a boom which extended forward from the left wing tip. (See Fig. 4). As has been previously stated, it was considered of prime importance that the sideslip measurement system have dynamic response characteristics such that no coupling error would be introduced.

Since no data were available for the response characteristics of the vane selected, theoretical calculations were made, and experimental tests conducted in order to determine if the natural frequency and damping ratio of the vane were within acceptable limits.

Theoretical Analysis

(See Ref. 1, pp 11.51-11.55). Notation as per sketch below.

V = true airspeed, ft/sec

V_i = indicated airspeed, ft/sec

M = moment about pivot

C_n = normal force coefficient

I = moment of inertia of vane

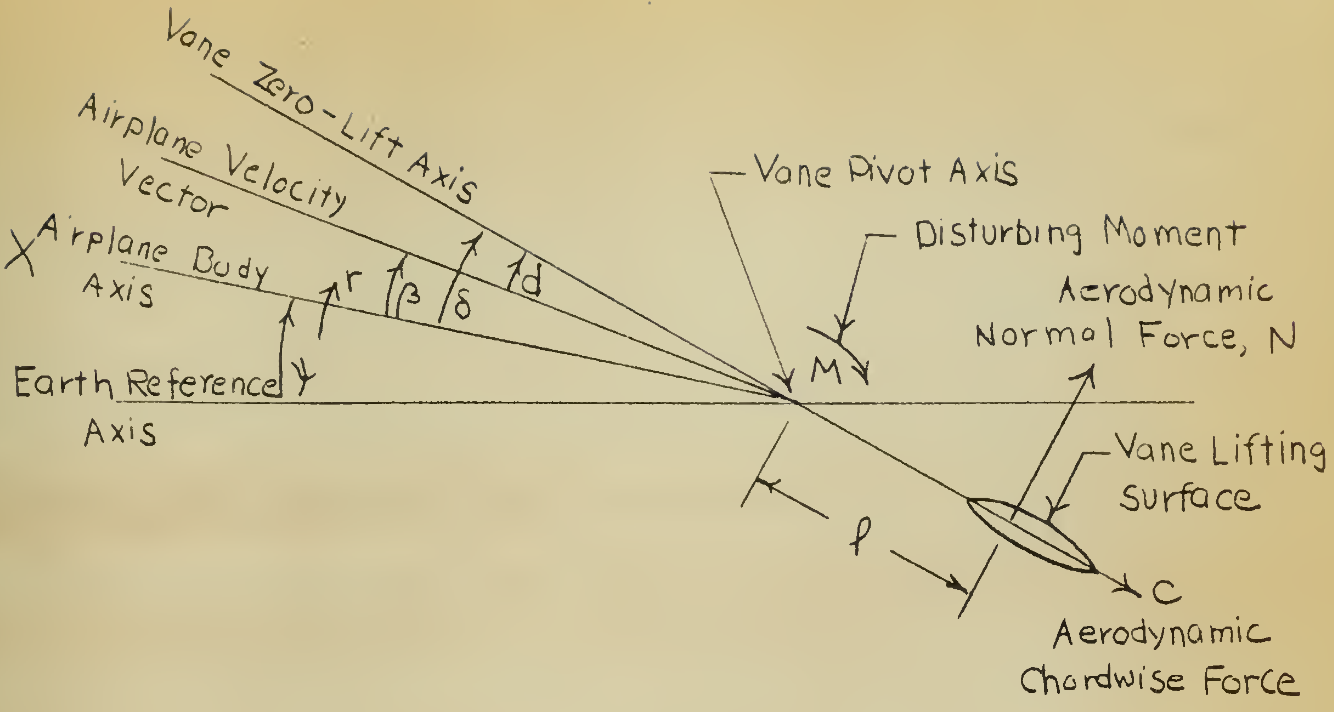

(1) $\alpha = \delta - \beta$ However, due to angular velocity of the vane with respect to the air mass, the angle of attack at the vane,

(2) $\alpha_v = \alpha + \frac{l}{V}(\dot{\delta} + r)$

(3) $\alpha_v = \delta - \beta + \frac{l}{V}\dot{\delta} + \frac{l}{V} r$

(4) $q = \frac{1}{2}\rho_0 V_i^2$, dynamic pressure

(5) $N = \frac{1}{2}\rho_0 V_i^2 S \alpha_v \frac{dC_N}{d\alpha}$

(6) $M - lN - (\ddot{\delta} + \dot{r}) = 0$

combining (3), (4), (5), & (6),

(7) $\ddot{\delta}\frac{1}{\omega_n^2} + \dot{\delta}\frac{2\zeta}{\omega_n} + \delta = \beta - r\frac{2\zeta}{\omega_n} - \dot{r}\frac{1}{\omega_n^2} + \frac{M}{K}$

where:

(8) $\omega_n = V_i \sqrt{\frac{\rho_0 S \ell}{2 I}\left(\frac{dC_N}{d\alpha}\right)}$ Natural Frequency of Vane

(9) $\zeta = \sqrt{\frac{\rho_0 \sigma S \ell^3}{8 I}\left(\frac{dC_N}{d\alpha}\right)}$ Damping Ratio of Vane

(10) $K = \frac{1}{2} S \rho_0 V_i^2 \ell \left(\frac{dC_N}{d\alpha}\right)$ Aerodynamic Stiffness of Vane

Conditions for Analysis:

Density Altitude: 5000 ft

V_i : 120 mph = 176 ft/sec

V : 189.6 ft/sec

S : .0361 ft^2

ℓ : .157 ft

$\frac{dC_N}{d\alpha}$: 1.72/radian (See Ref. 5)

I : 6.33×10^{-5} slug ft^2 (Determined experimentally)

From (8) above,

$$\omega_n = 176 \sqrt{\frac{.002378 \times .0361 \times .157 \times 1.72}{2 \times 6.33 \times 10^{-5}}}$$

$$\omega_n = 75.5 \frac{Ra}{sec}$$

$$f_n = \frac{\omega_n}{2\pi} = \underline{\underline{12.01 \text{ Cycles/sec}}}$$

From (9) above,

$$\zeta = \sqrt{\frac{.002378 \times .8616 \times .0361 \times (.157)^3 \times 1.72}{8 \times 6.33 \times 10^{-5}}}$$

$$= \underline{\underline{.031}}$$

Experimental Analysis

Since the above theoretical dynamic analysis of the response characteristics of the sideslip vane was based on a moment of inertia of limited accuracy, and neglected the effects of friction damping in the system, it was considered desirable to determine the dynamic response of the vane experimentally. Ref. 1 (p 11.55) reported that wind tunnel calibration of vanes is usually unsatisfactory because of the poorly-damped vane response to disturbances, and the usual high level of turbulence in wind tunnels. For this reason, the sideslip vane system was modified to permit in-flight dynamic testing of the vane when installed on the airplane. A spring and plunger mechanism, actuated by a solenoid, was installed on the boom, as indicated in Fig. 4. When in flight, operating at the desired test configuration, the vane was deflected by sideslipping the aircraft, and locked from the cockpit by electrically extending the plunger. (See Solenoid Switch, Fig. 3.) Thus, when the solenoid was reenergized, the vane was released, and responded as if to a step function. Fig. A-1 shows the transient response of the vane to such a step input. Calculations for the experimental determination of the natural frequency and damping ratio of the vane from the transient response of Fig. A-1 are as follows:

Conditions for Test

Density Altitude: 5000 ft

V_i : 120 mph $\simeq$ 176 ft/sec

In Ref. 6, it is shown that the undamped natural frequency and the damping ratio may be determined from transient data as follows:

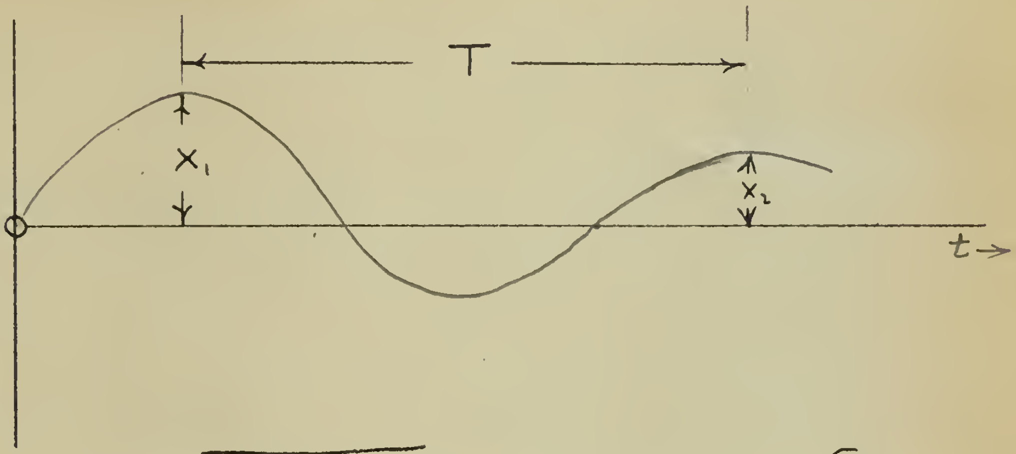

$$W_n = \frac{\sqrt{\delta^2 + \pi^2}}{T/2} \; ; \quad \zeta = \frac{\delta}{\sqrt{\delta^2+\pi^2}}$$

where

$$\delta = \ln \frac{X_2}{X_1} = \text{logarithmic decrement}$$

From Fig. A-1,

$$T = .065 \text{ sec.}, \quad X_1 = 4.0, \quad X_2 = 3.1$$

$$\delta = \ln \frac{4.0}{3.1} = .2546$$

$$\omega_n = \sqrt{\frac{(.2546)^2 + \pi^2}{.065/2}} = 97.0 \text{ Ra/sec.}$$

$$f_n = \frac{\omega_n}{2\pi} = \underline{\underline{15.44 \text{ Cycles/sec.}}}$$

$$\zeta = \sqrt{\frac{\delta^2}{\delta^2+\pi^2}} = \frac{.2546}{3.15} = \underline{\underline{.081}}$$

Comparison of Results

	Theoretical Analysis	Flight Test
fn, Natural Frequency cps	12.01	15.44
ζ, Damping Ratio	0.031	0.081

Concluding Remarks

(1) The natural frequency of the sideslip vane has been shown to be of the order of 16 cycles per second, and the damping ratio approximately 0.08.

(2) The ratio of the natural frequencies of the sideslip vane, and the airplane in the lateral oscillation is approximately 40.

(3) In view of (1) and (2) above, no dynamic correction to sideslip vane data was required.

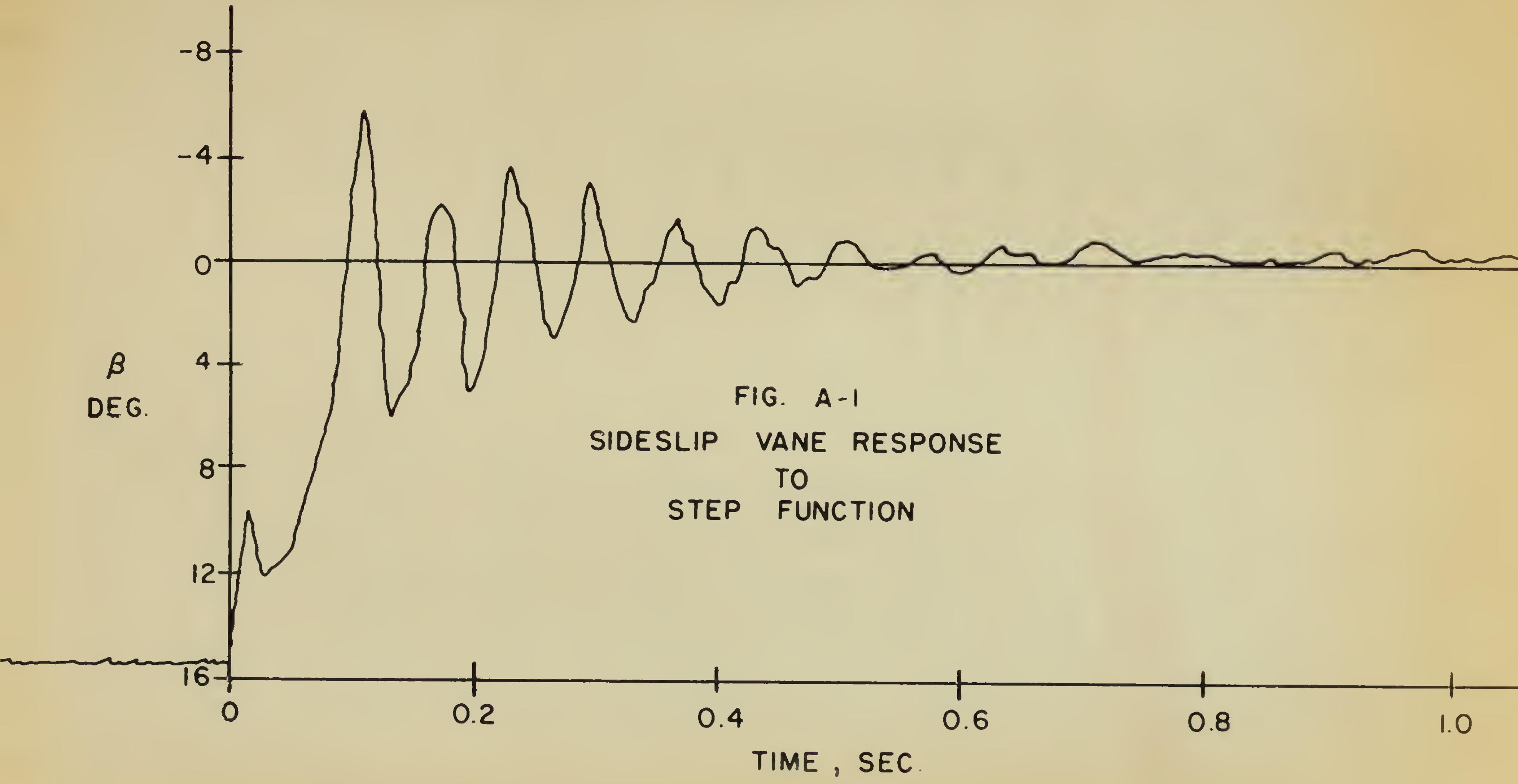

FIG. A-1
SIDESLIP VANE RESPONSE
TO
STEP FUNCTION

APPENDIX B

DETERMINATION OF LATERAL STABILITY DERIVATIVES FOR THE NORTH AMERICAN NAVION FROM THEORETICAL FORMULAE, AND FROM WIND TUNNEL AND FLIGHT TESTS FROM GEOMETRICALLY SIMILAR AIRPLANES

The determination of stability derivatives for an aircraft from theoretical and experimental data is a problem which has received widespread attention. Numerous publications, outlining a considerable number of methods for calculating or estimating derivatives, and presenting the results of extensive test programs, have appeared over the past twenty years. (See bibliography to Ref. 7). However, in spite of such a wealth of information on methods and test data, estimation methods are often found in practice to yield only fairly accurate values, suitable for making only first approximations to dynamic stability characteristics. In addition, the application of several theoretical methods to the same airplane often results in wide discrepancies between some of the calculated derivatives.

In general, the most reliable methods for calculation of lateral stability derivatives depend on wind tunnel data for accurate values of the sideslip derivatives, C_{Y_β}, C_{n_β}, & C_{l_β} . This is particularly true for propeller driven aircraft, where the propeller lateral force and slipstream effects are important contributions to the sideslip derivatives. No satisfactory purely theoretical method has yet been

developed for accurately estimating these derivatives for a complete airplane primarily because of large interference effects between the various airplane components.

The remarks above concerning wide discrepancies were found to be particularly pertinent to the calculation of the lateral stability derivatives of the North American NAVION. The derivatives for this airplane, including the sideslip derivatives, were calculated by five well known methods, and the results compared with test data, both for the NAVION, and also for several geometrically similar airplanes. The results, presented in Table B-II, showed a variation of at least 100% between the high and low values in the case of all derivatives with the exception of C_{l_p}, which varied by approximately 30%.

It is to be noted in Table B-II that the method of Ref. 5 gave the best correspondence between theoretically calculated derivatives, and the "average" derivatives of the several methods and tests results. Therefore, the detailed calculations for the lateral stability derivatives of the NAVION by the method of Ref. 5 are presented in the following pages.

GENERAL PARAMETERS FOR NORTH AMERICAN NAVION N91566

In addition to the physical characteristics of the NAVION presented in Table II to the basic report, the following parameters, determined from the assumed test conditions, are required for calculation of stability derivatives.

W	Gross weight during test, lb.	2770
h_d	Density altitude, ft	5000
ρ	Air density, slug/ft^3	.002049
V_i	Indicated airspeed, mph	120
V	True airspeed, ft/sec	189.6
C_L	Total lift coefficient	0.407
η_{VT}	Tail efficiency factor (estimated)	0.90

Unless otherwise specified, all further references in this appendix are to Ref. 5 to the basic report.

TABLE B-II (a)

THEORETICAL DETERMINATION OF THE LATERAL STABILITY DERIVATIVES OF NAVION N91566

Reference	(5) Perkins & Hage	(8) USNPGS Notes	(11) TR 635	(12) TR 589	(13) TN 1581	AVG. VALUE
C_{Y_β}	-.592*	-.592	-	-.632	-	-.612
C_{n_β}	.0613	.0708	-	.0409	-	.057
C_{l_β}	-.0816	-.1236	-.0981	-.1137	-.0991	-.107
C_{l_p}	-.46	-.495	-.46	-.46	-.304	-.44
C_{l_r}	.102	.110	-	.102	.0978	.103
C_{n_p}	-.051	-.0243	-	-.0431	-.0224	-.035
C_{n_r}	-.0937	-.0945	-	-.0953	-	-.095
$C_{Y_{\delta_r}}$	.111	-	-	-	-	.111
$C_{n_{\delta_a}}$	-.0087	-	-	-	-	-.0087
$C_{n_{\delta_r}}$	-.0561	-	-	-	-	-.0561
$C_{l_{\delta_a}}$	.133	-	-	-	-	.133

* From Ref. 8.

TABLE B II (b)

COMPARISON OF LATERAL STABILITY DERIVATIVES FOR AIRCRAFT GEOMETRICALLY SIMILAR TO NAVION N91566

REFERENCE	(9) P.R.* 232	(13) TN 2195	(14) TN 1327	(15) RM L53K09	(16) RM A52J06	AVG VALUE
C_L	.390	.334	.40	.33	.412	
S_{VT}/S_W	.068	.088	.185	.131	.10	
l_{VT}/b	.506	.460	.441	.456	.451	
AR	6.04	6.25	5.9	5.89	6.25	
λ	.527	.503	.500	.52	.576	
Γ, deg.	7.5	6.0	6.0	3.0	2.0	
Λ, deg.	0	0	0	0	0	
STABILITY DERIVATIVES						
C_{Y_β}	-.595	-.802	-.573	-.515	-.638	-.624
C_{n_β}	.141	.132	.0975	.1146	.109	.120
C_{l_β}	-.0822	-.08	-.0688	-.0573	-.078	-.073
C_{l_p}		-.43		-.39	-.476	-.432
C_{l_r}		.03		.06	.140	.073
C_{n_p}		-.007		-.02	-.020	-.018
C_{n_r}		-.160		-.13	-.138	-.143
$C_{Y_{\delta_r}}$	.203					.203
$C_{l_{\delta_r}}$	.0166					.0166
$C_{n_{\delta_r}}$	-.107					-.107
$C_{l_{\delta_a}}$	.101					.101
$C_{n_{\delta_a}}$	-.0035					-.0035

* For Navion 5113

C_{Y_β}

NOTE: Ref. 5 does not present a theoretical method for calculation of C_{Y_β}. Therefore, C_{Y_β} was calculated from the method of Ref. 8.

$$C_{Y_\beta} \approx -\frac{.12\,bL}{S} \qquad \text{where}$$

L = Fuselage length, Ft, ...27.25

$$C_{Y_\beta} = \frac{-.12\,(33.38)\,(27.25)}{184.2} = \underline{-.592}$$

C_{n_β}

Total directional stability, C_{n_β}, is composed of contributions from the wing, fuselage, propeller, vertical tail, and interference corrections due to wing configuration and to sidewash from the fuselage. In equation form,

$$\left(C_{n_\beta}\right)_{\text{airplane}} =$$

$$\left(C_{n_\beta}\right)_{\text{wing}} + \left(C_{n_\beta}\right)_{\text{fus}} + \left(C_{n_\beta}\right)_{\text{prop}} + \left(C_{n_\beta}\right)_{\text{vt}} + \Delta_1 C_{n_\beta} + \Delta_2 C_{n_\beta}$$

(a) $C_{n_{\beta_w}} = -.0006 \left| \Delta \right|^{\frac{1}{2}} \times 57.3 = 0$

(b) $\Delta_1 C_{n_\beta} = 0$ for low wing aircraft (see p. 320)

(c) $\underline{C_{n_\beta} \text{ fuselage}}$: An empirical relationship for this contribution, which is particularly applicable to single engined aircraft, is as follows:

$$C_{n_\beta \text{ fus.}} = .96 K_\beta \left(\frac{S_s}{S_w}\right)\left(\frac{L_f}{b}\right)\left(\frac{L_1}{L_2}\right)^{\frac{1}{2}}\left(\frac{W_2}{W_1}\right)^{1/3}$$

where

S_s = projected side area of fuselage in Ft^2

L_f = fuselage length

L_1, L_2, W_1, W_2 from accompanying sketch

K_β from Fig. 8-4, p. 320

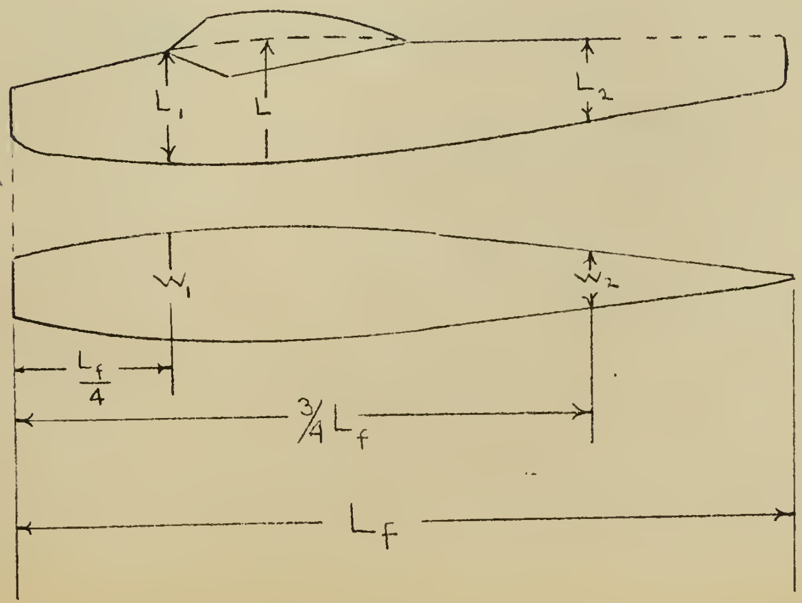

For the Navion, the above quantities are as follows:

S_s	ft^2	96.22
L_f,	ft	27.25
L_1,	ft	4.25
L_2,	ft	2.61
D_f,	ft	5.51
d_1,	ft	4.99
h_{max},	ft	4.40
W_1,	ft	4.14
W_2,	ft	1.76
d_2,	nose to c.g., ft	8.05
K_β,	(from Fig. 8-4)	.110

therefore,

$$C_{n_{\beta}\,\text{fuse}} = -(.96)\,(.110)\left(\frac{96.22}{184.2}\right)\left(\frac{27.25}{33.38}\right)\left(\frac{4.25}{2.61}\right)^{\frac{1}{2}}\left(\frac{1.76}{4.14}\right)^{\frac{1}{3}}$$

$$\underline{C_{n_{\beta}\,\text{fuse}} = -.0434}$$

(d) $\underline{C_{n_{\beta}\,\text{prop}}}$ from pp. 321,

$$C_{n_{\beta\,\text{Prop}}} = \frac{-\pi D^2 l_p \left(\frac{dC_{Y_p}}{d\psi}\right) N}{4 S_w b} \times 57.3$$

D = Propeller diameter, ft 7.0

N = Number of propellers 1

l_p = Distance from c.g. to propeller plane, ft, 7.90

$$\left(\frac{dC_{Y_\beta}}{d\psi}\right)_{T_c} = k\left(\frac{dC_{Y_\beta}}{d\psi}\right)_{T_c=0}$$ where, from p. 321,

$k = 1.5$ for full power,

$$\left(\frac{dC_{Y_\beta}}{d\psi}\right)_{T_c=0} = .00165 \text{ for two bladed propeller}$$

For Navion N91566 at full power,

$SHP = 185, \quad \eta_p = .632$ (Ref. 9)

$$T_c = \frac{550\,\eta_p\,SHP}{\rho V^3 D^2} = \frac{550 \times .632 \times 185}{.002049 \times (189.6)^3 \times (7)^2}$$

$$T_{c\ \text{full power}} = \underline{.0940}$$

For cruise power,

$SHP = 130, \quad \eta_p = .78$

$$T_c = \frac{550 \times .78 \times 130}{.002049 \times (189.6)^3 \times (.7)^2} = .0815$$

$$k_{\text{cruise power}} = \frac{T_{c\ \text{cruise power}}}{T_{c\ \text{full power}}} \times (1.5)$$

$$h_{\text{cruise power}} = \frac{.0815}{.0940} \times 1.5 = \underline{1.3}$$

$$\left(\frac{dC_{Y_\beta}}{d\psi}\right)_{\text{cruise power}} = 1.3\ (.00165) = \underline{.00214}$$

$$C_{n_\beta\ \text{prop}} = \frac{-\pi\,(7)^2\,(7.90)\,(.00214)\,(1)\,(57.3)}{4 \times 184.2 \times 33.38}$$

$$C_{n_\beta\ \text{prop}} = \underline{-.00610}$$

(e) C_{n_β} vertical tail

$$C_{n_\beta\,vt} = a_{vt} \frac{S_{vt}}{S_w} \frac{\ell_{vt}}{b} \eta_{vt}$$

a_{vt}, the slope of the side force curve for the vertical tail, is a function of the effective aspect ratio of the vertical tail, AR_e.

From p. 325,

$AR_e = 1.55 \dfrac{b_{vt}^2}{S_{vt}}$ where S_{vt} is the nominal vertical tail area as indicated on p. 325.

$$AR_{e\,Navion} = \frac{1.55 \times (4.05)^2}{10.89} = 2.33$$

From Fig. 8-8, p. 324,

$a_{vt} = .048/\text{deg} = 2.75/\text{radian}$

ℓ_{vt} = distance from airplane c.g. to aerodynamic center of the vertical tail.

As measured from a scale drawing for appropriate c.g.,

$$\ell_{vt\,Navion} = 16.88 \text{ Ft.}$$

$\eta_{vt} = \dfrac{q}{q_o}$; assumed = .90

When sidewash effects are included as a part of the tail efficiency factor instead of as an increment, $\Delta_2 C_{n_\beta}$, the total efficiency factor can exceed unity, and is of the form:

$\left(1 - \dfrac{d\sigma}{d\psi}\right) \eta_{vt}$ See for example, Fig. 21a of Ref. 10.

$$C_{n_\beta\,vt} = 2.75 \frac{(12.925)}{(184.2)} \frac{(16.88)}{(33.38)} (.9)$$

$$C_{n_\beta\,vt} = \underline{.0877}$$

(f) $\Delta_2 C_{n_\beta}$, sidewash or interference flow correction due to wing-fuselage combination.

From Fig. 8-7, p. 325, with D_f and d, from part (c) above:

$$d_1/D_f = \frac{4.99}{5.51} = .904$$

$$\Delta_2 C_{n_\beta} = .0004 \times 57.3 = \underline{.0229}$$

therefore,

$$C_{n_\beta} = C_{n_{\beta_{wing}}} + C_{n_{\beta_{fus}}} + \Delta_1 C_{n_\beta} + C_{n_{\beta_{prop}}} + C_{n_{\beta_{vt}}} + \Delta_2 C_{n_\beta}$$

$$= 0 - .0434 + 0 - .0061 + .0877 + .0229$$

$$\underline{\underline{C_{n_\beta} = .0613}}$$

$$\underline{C_{l_\beta}}$$

$$C_{l_{\beta}\,airplane} = C_{l_{\beta_{wing}}} + C_{l_{\beta_{vert.\ tail}}} + \Delta_1 C_{l_\beta} + \Delta_2 C_{l_\beta}$$

where

$\Delta_1 C_{l_\beta}$ is a correction for wing-fuselage interference due to wing height.

$\Delta_2 C_{l_\beta}$ is a correction for wing-vertical tail interference as a function of wing height.

The effects of power on C_{l_β} are negligible for the "clean" condition.

(a) $\underline{C_{l_\beta}\text{ wing:}}$ (See Fig. 9-3, p. 344)

For $AR = 6$ Extent of dihedral

$\lambda = .5$ $= 1.0,$

$$\frac{C_{l_\beta}}{\Gamma}\text{ wing, due to }\Gamma = -.74/\text{radian}$$

$$C_{l_\beta}\text{ wing} = \frac{-.74 \times 7.5}{57.3} = -.0968/\text{ra.}$$

$$\Delta C_{l_\beta}\text{ tipshape} = 0,\text{ from Fig. 9-5, p. 345.}$$

(b) $\Delta_1 C_{l_\beta}$: From Eqn. 9-6, p. 347,

$$\Delta_1 C_{l_\beta}\text{ low wing} = .0008 \times 57.3 = \underline{.0458}$$

(c) C_{l_β} vertical tail:

$$C_{l_\beta}\text{ vertical tail} = -a_{vt}\,\frac{S_{vt}}{S_w}\,\frac{Z_{vt}}{b}\,\eta_{vt}$$

where Z_{vt} = distance from X axis to aerodynamic center of vertical tail.

Z_{vt} for Navion = 4.10 Ft.

$$C_{l_\beta\, vt} = -2.75\,\frac{(12.925)}{(184.2)}\,\frac{(4.10)}{(33.38)}\,(0.90)$$

$$C_{l_\beta\, vt} = -.0214/\text{ra}$$

(d) $\Delta_2 C_{l_\beta}$: From Eqn. 9-11, p. 346:

$$\Delta_2 C_{l_\beta}\text{ low wing} = -.00016 \times 57.3$$

$$\Delta_2 C_{l_\beta}\text{ low wing} = \underline{\underline{-.00916}}$$

$$C_{l_\beta \text{ airplane}} = C_{l_\beta \text{ wing}} + C_{l_\beta \text{ vt}} + \Delta_1 C_{l_\beta} + \Delta_2 C_{l_\beta}$$

$$= -.0968 \quad -.0214 \quad + .0458 \quad -.00916$$

$$C_{l_\beta} \text{ airplane} = \underline{\underline{-.0816}}/\text{ra}$$

C_{l_p}, Damping in Roll

See Fig. 9-14, p. 351.

For $\lambda = 0.5$, $AR = 6.04$,

$$C_{l_p} \text{ Navion} = \underline{\underline{-.46}}$$

Referring to pp. 428-429

C_{l_r}, Roll Due to Yaw

By strip integration, and assuming elliptical lift distribution,

$$C_{l_r} = \frac{C_L}{4} = \frac{.407}{4} = \underline{\underline{.102}}$$

C_{n_p}, Yaw Due to Roll

$C_{n_p} = -\frac{C_L}{8}$, also by strip integration and for elliptical lift distribution.

$$C_{n_p \text{ Navion}} = -\frac{.407}{8} = \underline{\underline{-.051}}$$

C_{n_r}, Damping in Yaw

$$C_{n_r} = -\frac{C_{D_W}}{4} - 2a_{vt}\frac{S_{vt}}{S_w}\left(\frac{\ell_{vt}}{b}\right)^2 \eta_{vt}$$

C_{D_W}: From p. 95,

$$C_{D_W} = C_{D_{W_o}} + \frac{C_L^2}{\pi \mathcal{R} e}$$

$C_{D_{W_o}} = .008$

$\mathcal{R} = 6.04$

$e = .78$

$C_{D_W} = .008 + .07\, C_L^2$

For $C_L = .407$, $C_{D_W} = .0196$

$$C_{n_r} = -\frac{.0196}{4} - 2 \times (2.75) \times \frac{(12.925)}{(184.2)}\left(\frac{16.88}{33.38}\right)^2 (.9)$$

$$= -.0049 - .0888$$

$$C_{n_r} = \underline{\underline{-.0937}}$$

$C_{n_{\delta r}}$

$$C_{n_{\delta r}} = -a_{vt}\,\tau_r \frac{S_{vt}}{S_w} \frac{\ell_{vt}}{b} \eta_{vt}$$

where τ = rudder effectiveness,

From Fig. 5-33, p. 250

$$\frac{S_{rudder}}{S_{vt}} = \frac{6.052}{12.925} = .469$$

$$\tau_r = .64$$

$$C_{n_{\delta r}} = -2.75\ (.64)\ \frac{(12.925)}{(184.2)} \left(\frac{16.88}{33.38}\right) (0.9)$$

$$C_{n_{\delta r}} = \underline{\underline{-.0561}}$$

$C_{\ell_{\delta r}}$

$$C_{\ell_{\delta r}} = \frac{-h_{vt}}{\ell_{vt}} C_{n_{\delta r}}$$

$\frac{h_{vt}}{\ell_{vt}}$ Navion From Ref. 9 = .155

$$C_{\ell_{\delta r}} = -.155\ (-.0561) = \underline{\underline{.0087}}$$

$C_{Y_{\delta r}}$

$$C_{Y_{\delta r}} = -\frac{b}{\ell_{vt}} C_{n_{\delta r}} = \frac{-(33.38)}{(16.88)} (-.0561)$$

$$= \underline{\underline{.111}}$$

$C_{l_{\delta a}}$

$$C_{l_{\delta a}} = \tau_a \times \left(\frac{C_{l_{\delta a}}}{\tau_a}\right)$$ where

τ_a = aileron effectiveness, a function of aileron-wing chord ratios.

$\left(\frac{C_{l_{\delta a}}}{\tau_a}\right)$ is a function of the location of the inboard and outboard ends of the aileron in percent of semispan. (See Fig. 9-3, p. 344.)

$$\frac{\text{Aileron inboard end}}{b/2} = \frac{7.74}{11.93} = .649$$

$$\frac{C_{l_{\delta a}}}{\tau_a} = .42$$

$$\frac{\text{Aileron outboard end}}{b/2} = \frac{11.4}{11.93} = .955$$

$$\frac{C_{l_{\delta a}}}{\tau_a} = .70$$

$$\text{Net } \frac{C_{l_{\delta a}}}{\tau_a} = .70 - .42 = \underline{.28}$$

From Fig. 9-15, p. 358,

For $\frac{c_a}{c_w} = .284$, and for

Frise ailerons, $\tau_a = .475$

$$C_{l_{\delta a}} = .475 \times .28$$

$$C_{l_{\delta a}} = \underline{\underline{.133}}$$

J_x, J_z

$$J_x \equiv 2\left(\frac{k_x}{b}\right)^2 ; \quad k_x^2 \equiv \frac{I_x}{m}$$

$$J_z \equiv 2\left(\frac{k_z}{b}\right)^2 ; \quad k_z^2 \equiv \frac{I_z}{m}$$

From Ref. 3, for the Navion,

I_x = 1060 slug-ft^2

I_z = 3552 slug-ft^2

W = 2770 lb.

$$J_x = \frac{2\,I_x}{m\,b^2} = \frac{2 \times 1060}{2770/32.2\ (33.38)^2} = \underline{\underline{.0222}}$$

$$J_z = \frac{2\,I_z}{m\,b^2} = \frac{2 \times 3552}{2770/32.2\ (33.38)^2} = \underline{\underline{.0745}}$$

APPENDIX C

CORRECTIONS TO RECORDED AILERON DATA

During preliminary matching of responses of the test aircraft and the computer to aileron forcing functions, it was determined that the recorded values of aileron position angle would require correction for errors introduced as a result of a combination of aileron cable stretch and a non-linear hinge moment curve. In order to quantitatively establish the extent of the required correction, the computer problem was forced by an aileron step input to the left and the roll rate response matched to the flight data by adjusting $C_{l_{\delta_a}}$; a similar aileron input to the right was then introduced, and was observed to cause a computer response in roll rate that was smaller than the flight data by a factor of 0.78. This factor of 0.78 was proved to remain constant over a wide range of values of C_{l_p}, the one stability derivative that would have a marked effect on the roll rate due to aileron deflection. Similarly, the roll response to an aileron doublet could be brought into perfect match with the flight data during the initial roll to the left, but no reasonable value of C_{l_p} would produce as high a roll rate to the right as was recorded in the flight data. (Values of C_{l_p} as low as 0.28 were investigated.)

At this point, equation (9-33) of Ref. 5 was rewritten in ratio form, and applied to responses of actual flight data of aileron step

functions to the right and left, as follows:

$$\frac{\dot{\phi}\ \text{left}}{\dot{\phi}\ \text{right}} = k\,\frac{\delta_a\ \text{left}}{\delta_a\ \text{right}}$$

The k factor was inserted in the equation knowing that its value should be unity. However, upon solving for k it was again determined to be the factor 0.78.

This analysis offered sufficient proof that an instrumentation error had been included in the data. The gyro measuring the roll rate response was known to be highly accurate, but aileron deflection was measured directly at the right aileron and the calibration curve was obtained on the ground under a no-load condition. Aileron cable stretch was known to exist to some degree in the aircraft used, and for this reason, aileron deflection was measured directly at the right aileron. Instead of alleviating the instrumentation error, however, this merely caused it to be additive during left roll and subtractive during right roll. This condition can be demonstrated by first considering the non-linear hinge moment characteristic of a modified frise aileron:

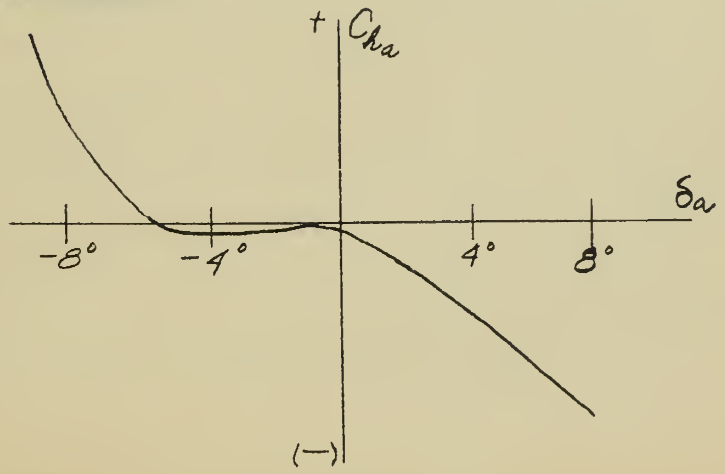

It should be noted that the change in hinge moment is nearly proportional to the deflection when the aileron is displaced down. Therefore, due to cable stretch, the down-going aileron would be attenuated by a constant factor in comparison to the no-load calibration. The up-going aileron has a relatively constant hinge moment over the range used in this investigation and would therefore parallel the no-load calibration curve. The resulting error is illustrated by a plot of control deflection vs. aileron deflection:

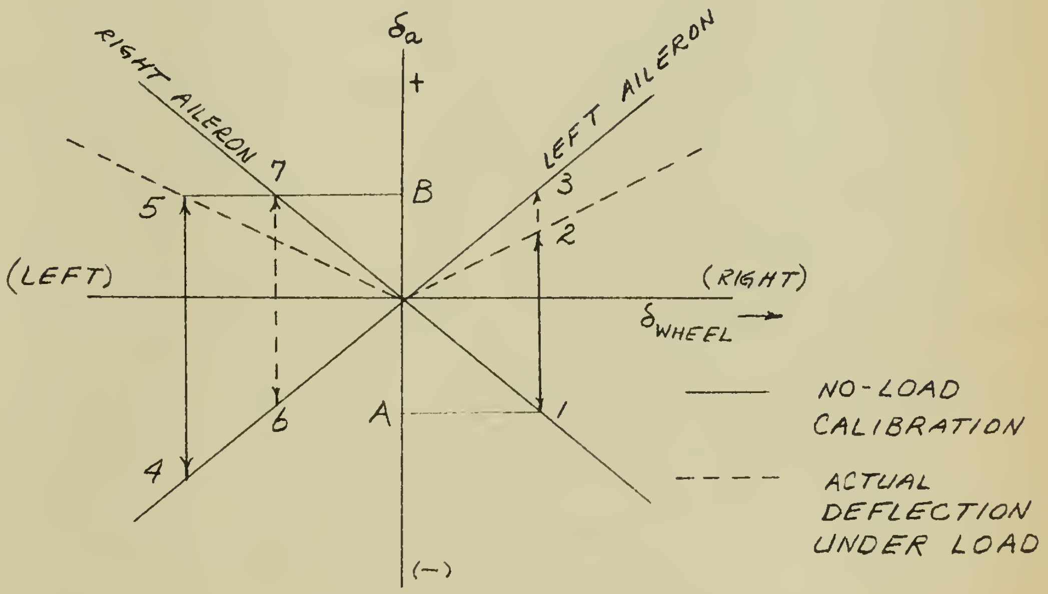

When the ailerons are deflected to the point where the right aileron is at position A, the signal output is proportional to the length 1 - 3, but the actual deflection is the shorter length 1 - 2. Correspondingly, if the controls are reversed to the point where the right aileron is at point B, the signal output is proportional to the length 6 - 7, but the true position is then the larger value 4 - 5.

Qualitatively, this discussion would hold true whenever the slope of the hinge moment curve differs between the up-going aileron and the down-going aileron. Although no hinge-moment data was available for the Navion, the ailerons are of the modified frise type, which are known to have this characteristic.

Having qualitatively explained the error in terms of non-linear hinge moments, and having quantitatively found the magnitude of the error both from flight data analysis and from the computer responses to aileron step functions, it then became necessary to remove the error from the signal in order to continue the computer analysis. Although the ailerons had a differential gearing characteristic for large deflections which would affect the apportionment of the error between the right and left signals, the differential effect was less than ten percent in the small range of deflections used, and thus the apportionment of the error could be made on a 50-50 basis with reasonable assurance. (This concept could be verified by making reference to the plot of control deflection vs. aileron deflection. With no differential in the aileron system, the percent of error for a given control deflection to the left is equal to the percent of error for a corresponding control deflection to the right, but the signs of the errors are opposite. Adding a differential gearing effect changes this equality between the error signals, but not to a marked degree.)

To effect the change in the aileron signal, circuitry was provided

to divide the signal into two paths, one path for the signal during right roll, and another path for the signal during left roll. The right roll signal was then attenuated by the previously established factor of 0.78. This circuitry is shown in Fig. 9.

With this change the character of the signal had been corrected, but the magnitude of the entire signal was known to be low because the correction had all been placed in one direction as an attenuation rather than being apportioned evenly between the two directions of roll as an attenuation of one and as amplification of the other. The amount by which the signal was low was the ratio of 0.78/0.89, or (0.877), for dividing the signal by that factor would halve the previous attenuation in the right signal and amplify the left signal correspondingly. Thus the correction would be apportioned equally to the two signals:

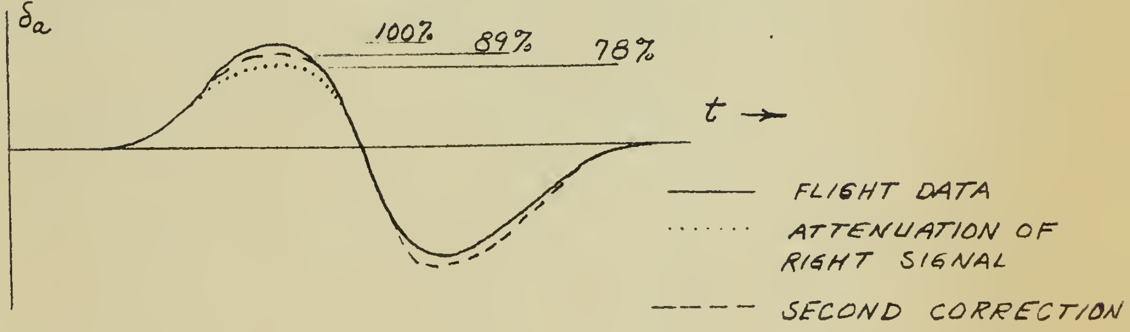

Instead of applying this second correction factor to the signal which would have required additional changes in the circuitry, the investigation was carried to its conclusion and the correction factor was then inversely applied to the value of the aileron derivatives, the net effect

of the two alternative methods of correction being identical in the final result.

In conclusion, it should be stated that the corrections made to the signal were justified by the viewpoints brought out in the above discussion. However, to state that the error was completely eliminated would seem overly optimistic, especially with respect to the apportionment between attenuation of the signal in one direction and amplification of the signal in the other direction. It is strongly felt, however, that any error remaining in the aileron signal had no effect on the value of any of the derivatives other than the aileron derivatives, $C_{l_{\delta a}}$ and $C_{n_{\delta a}}$. The magnitude of the error produced in these two derivatives should not exceed five to eight percent.

A more suitable method of instrumentation would have been to include a transducer at each aileron, and sum the two aileron angle signals and compute the average angle as a function of time on the analog computer.

An investigation of the feasibility of obtaining lateral stability derivatives for a linea aircraft by matching analog computer transient responses to flight test data

Thesis 35762
A233 Adams
An investigation of the feasibility of obtaining lateral stability derivatives for a linear aircraft by matching analog computer transient responses to flight test data.